

**POLITECNICO DI TORINO**

**Master's Degree in Mechanical Engineering**

Master of Science in Mechanical Engineering Thesis

**Processing of Waste-Water Sludge for Energy Recovery and  
Cement Production**



**Tutors**

Prof. Marco Carlo Masoero

Prof. Marta Gandiglio

**Candidate**

Sina Attari

December 2021



## **Abstract**

Sewage sludge from municipal wastewater treatment plants is currently being disposed of with thermal treatment and agricultural utilization or landscaping. Increasing focus on hygiene and soil protection combined with the new legal developments leads to the increased relevance of thermal sewage sludge treatment processes. In this thesis, a sustainable solution of thermal drying and disposal of sewage sludge by co-incineration in cement rotary kiln which is encouraged by Cementi Victoria s.r.l. will be introduced.

The thesis is divided into different parts that follow the chronological order of development of the thesis. After a brief presentation of the cement production process in Cementi Victoria s.r.l, a review of methods that can be potentially utilized to dry the municipal sewage sludge and some other industrial experiences of the dried sewage sludge (DSS) usage in cement industries had been introduced. Finally, a computational fluid dynamics (CFD) method was used to investigate the possibility of DSS co-incineration as a secondary fuel inside a cement rotary kiln.

**Keywords:** sewage sludge disposal (SSD), sewage sludge drying, thermal recovery of flue gases, cement rotary kiln, dried sewage sludge (DSS) co-incineration, computational fluid dynamics (CFD).



## **Acknowledgment**

I would like to take this opportunity to extend my appreciation to everyone who has supported me throughout the development and completion of my thesis. I would particularly like to thank my supervisor Professor Marco Carlo Masoero for his availability by allocating his time, for his expertise and knowledge in clarifying my doubts, and for his guidance and advice. The guidance and inputs provided by him served as an invaluable part in the completion of my thesis work.

I would like to acknowledge my family who has always been there for me despite the distance. I would like to make special mention of my mother and father, who has always been my pillar of mental support.



# Contents

1	Introduction .....	1
2	The cement factory .....	2
2.1	Production process of cement .....	3
2.1.1	Crushing of the raw material .....	3
2.1.2	Raw grinding .....	3
2.1.3	Cooking process .....	4
2.1.4	Grinding of terracotta .....	5
2.1.5	Bagging and loading.....	5
2.1.6	Tests and checks .....	5
2.2	Environmental impacts .....	6
2.2.1	Cooling tower .....	6
3	Literature Review .....	8
3.1	Sewage sludge drying modes.....	8
3.1.1	Convective drying .....	9
3.1.2	Conductive drying .....	9
3.1.3	Solar drying .....	9
3.2	Sewage sludge innovative drying methods.....	10
3.2.1	Convective-conductive drying powered by a WTE power plant flue gas.....	10
3.2.2	Convective-conductive drying powered by a heat pump .....	11
3.2.3	Solar-conductive drying powered by a heat pump and solar energy.....	12
3.2.4	Convective drying powered by geothermal energy .....	13
3.2.5	Convective drying powered by CHP units fueled by natural gas.....	14
3.2.6	Convective drying powered by a CHP unit fueled by biogas-natural gas.....	16
3.2.7	Convective drying powered by a CHP unit fueled by syngas-WVO .....	17
3.3	Sewage sludge drying practices in cement plants.....	19
3.3.1	Cemex, Alicante .....	19
3.3.2	Schwenk, Allmendingen.....	20
3.3.3	Wietersdorfer, Wietersdorf.....	20
3.3.4	Würenlingen, Switzerland .....	20
3.3.5	Huangshi, Huaxin .....	21
3.3.6	Schwenk, Karlstadt.....	21
3.4	Sewage sludge co-firing on cement plants .....	25
3.4.1	Sewage sludge firing in the kiln burner.....	26
3.4.2	Sewage sludge firing in the calciner burner .....	37

3.5	Eco-cement quality when DSS added to raw materials .....	40
3.6	Eco-cement quality when DSS Ash added to raw materials .....	41
3.7	Flue gas treatment .....	42
4	Case study .....	43
4.1	Evaluation of the LHV of SS provided by Cuneo WWTP.....	43
4.2	A proposal for drying of SS in case of Cementi Victoria s.r.l. ....	45
4.3	Burner replacement .....	48
4.4	Fuels .....	50
4.4.1	DSS combustion kinetics .....	51
4.4.2	petcoke combustion kinetics .....	53
4.5	CFD analysis .....	55
4.5.1	Geometry.....	55
4.5.2	Meshing.....	55
4.5.3	Setup.....	56
4.5.4	Results and discussion .....	57
5	Conclusion .....	59
6	References.....	60

## List of figures

Figure 1 Cementi Victoria .....	2
Figure 2 Hybrid convective-conductive drying powered by a WTE power plant flue gas .....	11
Figure 3 Hybrid convective-conductive drying powered by a heat pump .....	11
Figure 4 Hybrid drier with two conveyors .....	12
Figure 5 hybrid solar-conductive drying powered by a heat pump and solar energy .....	12
Figure 6 Convective drying powered by geothermal energy .....	14
Figure 7 Schematic diagram of a belt drying system assisted by CHP units .....	16
Figure 8 Convective drying powered by a CHP unit fueled by biogas and natural gas .....	17
Figure 9 Convective drying powered by a CHP unit fueled by syngas and WVO .....	18
Figure 10 Schematic diagram of the SS management process in Cemex, Alicante .....	20
Figure 11 Schematic of SS management process in Würenlingen, Switzerland .....	21
Figure 12 Schematic diagram of SS drying and usage process in Schwenk, Karlstadt .....	22
Figure 13 Flowsheet of the waste heat recovery plant in Schwenk, Karlstadt .....	23
Figure 14 Belt drier design for the sewage sludge drying in Schwenk, Karlstadt .....	24
Figure 15 Flowsheet of the chemical scrubber and the biofilter in Schwenk, Karlstadt .....	25
Figure 16 DUOFLEX™ G2 from FLSmidth .....	28
Figure 17 ROTAFLAM® .....	28
Figure 18 PYROSTREAM® .....	29
Figure 19 POLFLAME® .....	29
Figure 20 FLEXIFLAME™ .....	30
Figure 21 Mono-Air duct-System .....	30
Figure 22 A schematic overview of the in-line separate calciner cement pyro-system .....	33
Figure 23 Kiln shell temperature profile before DSS firing .....	35
Figure 24 Kiln shell temperature profile with 2 t/h of DSS firing with velocity 48.5 m/s .....	36
Figure 25 Kiln shell temperature profile with 2.7 t/h of DSS firing with velocity 30 m/s .....	36
Figure 26 Schematic presentation of the cement manufacturing process .....	38
Figure 27 The effect of the sludge feed method on NO <sub>x</sub> and CO emission .....	40
Figure 28 The effect of the sludge feed method on O <sub>2</sub> emission .....	40
Figure 29 Greenhouse dryer .....	46
Figure 30 Radiant floor composition .....	46
Figure 31 Huber belt dryer BT .....	47
Figure 32 ROTAFLAM® KGO burner from Pillard Feuerungen GmbH .....	49
Figure 33 Dimensioning of the new ROTAFLAM® KGO burner face .....	49
Figure 34 Rotary kiln and burner after meshing in ANSYS MESHING TOOL .....	56
Figure 35 Flame shape and temperature .....	57
Figure 36 Char burn out quantity and path .....	58

## List of tables

Table 1 Characteristics and operation parameters of selected driers .....	8
Table 2 Main design parameters and performance data of the belt drier.....	15
Table 3 Dried sewage sludge usage in some cement industries .....	19
Table 4 Industrial rotary kiln burners for cement industry, AF alternative fuels .....	31
Table 5 Fuel analysis on as received (a.r.) and dry-ash-free (daf) mass basis.....	33
Table 6 Cement plant operation points during sewage sludge firing trials.....	34
Table 7 The chemical composition (wt.%) of cement produced with and without SS as fuel	39
Table 8 The mineral composition (wt.%) of cement produced with and without SS as fuel ..	39
Table 9 The effect of feed point on NO <sub>x</sub> , CO, and O <sub>2</sub> emission at the feed rate of 9 t/h .....	39
Table 10 Feed rate of dried sludge in the different series .....	39
Table 11 Water and TOC content of the dewatered SS provided by Cuneo WWTP .....	44
Table 12 LHVs of the SS provided by Cuneo WWTP (dry basis) .....	45
Table 13 Solar drying greenhouse versus convective drying belt dryer .....	48
Table 14 Ultimate and proximate composition of the chosen DSS .....	50
Table 15 Ultimate and proximate composition of the chosen petcoke .....	50

# 1 Introduction

This work, carried out in the context of a collaboration with the Cementi Victoria s.r.l., was created to investigate the company's interest in the sludge disposal sector.

The production of sludge deriving from the treatment of urban wastewater has been growing in recent years thanks to an improvement in the purification capacity of the individual plants. The European Community is proving to be increasingly sensitive to environmental impact and sludge disposal is a topic of great current interest.

The goal is to make the sludge suitable for final disposal at the lowest cost and to encourage its recovery. This waste can be disposed of in landfills, incinerated with or without energy production, recovered in agriculture as fertilizer, or finally reused in the production of bricks, asphalt, and concrete. The indications and obligations deriving from recent regulations provide for more complex management of mud from an operational and administrative point of view. Disposal in controlled landfills now requires the same stabilization and dehydration treatments necessary for the reuse of sludge as soil improvers for agricultural use.

The difficulty of creating new landfills on the regional territory is generating widespread interest among the managers of purification plants to consider alternative locations, such as use in agriculture, sending to composting, and combustion plants.

In recent years it has been learned that the revaluation of this waste in agriculture is not harmless: it has been ascertained an enrichment of heavy metals in the land. Furthermore, the sludge is contaminated to varying degrees by pathogenic microorganisms. The introduction of stricter limits, combined with the increasing attention of public opinion on the quality of the environment, is imposing more stringent treatment levels as well as a reduction in the spreading activity itself on the ground.

The disposal of these substances has become an increasingly difficult road to follow, and this has prompted plant managers to evaluate the thermal drying process aimed at removing the liquid phase from the sludge. The amount of water present in the sludge, which can be up to 97%, is a key factor in cost planning. Only dried sludge can be transported and disposed of economically. Furthermore, reaching a dry content close to 90%, the sludge could be used as an alternative fuel for energy production (waste-to-energy).

Based on these considerations, the Cementi Victoria s.r.l. intends to combine the production of cement with the thermal drying of the sludge. The production process of the cement factory is characterized by a large amount of waste heat; the combustion that takes place in the rotary kiln for the clinker production (the raw material of cement) produces hot fumes at a temperature of 360-400 °C. The goal of the thesis work is therefore to find the best solution for the recovery of thermal waste to carry out a sludge drying process. In the following paragraphs, more common ways of drying methods will be discussed, and a more efficient solution will be introduced. Finally, a feasibility analysis of using DSS (Dried Sewage Sludge) as a secondary fuel and/or a raw material for the production process of clinker will be investigated.

## 2 The cement factory

The Cementi Victoria s.r.l., born in Trino (VC) in 1935, is one of the smallest companies operating in the Italian cement industry. A family-run company now in its third generation, it is classified among the units with the lowest production (lower than 100,000 t/year). Unlike many competitors in the sector, it boasts a complete production cycle: the raw material, calcareous marl, is taken from a proprietary quarry located at about 20 km and then transported to the plant where it is suitably crushed, mixed with other high-grade materials. Calcium carbonate content  $\text{CaCO}_3$  is from Bergamo and fired in an Ansaldo Smidth type 82 m rotary kiln for clinker production (product obtained by firing limestone and clay, basic component for the cement production). The clinker is then mixed and ground with other materials (e.g., limestone, gypsum, silica, fly ash, slag, and pozzolan) to obtain two types of cement: [1]

- Portland composite cement (EN 197-1) Type II /B-M (PL) 32.5 R
- Portland composite cement (EN 197-1) Type II /A-M (PL) 43.5 R

Type II/A cement has a clinker content greater than 80%, while type II / B cement is produced with clinker percentages greater than 65%. Cement is sold both in bulk and bagged. About 80% of the production is intended for sale in bags due to the absence of large consumer customers. The main buyers are warehouses and small businesses. The small size of the plant makes it possible to take greater care of the quality of the product since the control and intervention for any anomalies is more immediate but at the same time involves more charges and high unit costs compared to the large Italian cement groups, both for the high load of manpower and for the incidence of maintenance costs since it is a cement industry with great wear and tear of machinery. Figure 1 shows Cementi Victoria s.r.l. plant [1].



Figure 1 Cementi Victoria

The company has always shown a great interest in alternative energy: in the plant, there is a photovoltaic system equipped with solar trackers with producibility of approximately 200,000 kWh/year which corresponds to approximately 4% of the needs of the cement factory [1].

## **2.1 Production process of cement**

The Trino (VC) cement factory of the company Cementi Victoria s.r.l. is a factory that produces hydraulic binders that comply with the UNI EN 197-1: 2007 and UNI EN 197/2 standards. Cement is produced from clinker manufactured in the cement factory and from constituents added in grinding such as limestone, pozzolanic materials, powders, and gypsum. The production capacity is approximately 60,000 t/year clinkers and 80,000 t/year of cement. The plant has about 30 employees. Many jobs, such as quarrying and transport, are outsourced. The management of the plant plans the production processes for quality and quantity following the company objectives. Given the ever-increasing difficulties in finding raw materials, such as limestone and pozzolanic clay, due to the impossibility of opening new quarries, in recent years the cement factory has started tests with raw-secondary materials to make up for the lack mainly of high-content calcareous marl of calcium carbonate  $\text{CaCO}_3$ . These materials are stored in the yard together with the raw material, mixed with it, and sent to the hopper in the mill for the crushing process. Being high humid materials, dehumidification is necessary, carried out with the hot fumes coming from the kiln [1].

The activities of excavation and transport to the cement factory of raw materials are entrusted to third parties. The main raw materials used in the plant are calcareous and clayey marl, calcium carbonate  $\text{CaCO}_3$ , silica  $\text{SiO}_2$ , calcium sulfate  $\text{CaSO}_4$ , and pozzolan. These once arrived in the factory, are identified, and weighed, subsequently crushed, or stored. The main phases in which the production process is divided are described below [1].

### **2.1.1 Crushing of the raw material**

A plate conveyor collects the material (calcareous and clayey marl) from the unloading hopper and sends it to a vibrating screen for sieving to a sorting plane, consisting of interchangeable bars, operated by an 11 KW electric motor, whose potential is about 60 t/h of clayey limestone in size 0-700 mm with a maximum humidity of 18%. The material then arrives at the crusher whose potential varies between 40-60 t/h depending on the type of material processed. The maximum output size can reach up to about 40 mm. The crushed material is stored in a shed and subsequently taken underground using milling extraction systems, to then be sent to the mill for grinding. The stored raw material contained  $\text{CaCO}_3$  not less than 70%. Further corrections to bring the count with  $\text{CaCO}_3$  to 75% are made on the feeding belt for the grinding mill, with volumetric dosing plates fed by  $\text{CaCO}_3$  storage silos with a purity higher than 95% [1].

### **2.1.2 Raw grinding**

This phase of the process consists of the dosage, drying, and grinding of the raw materials, obtained from the excavation process and subsequent homogenization in the crushing hopper according to the indications provided by the Central Laboratory of the cement factory. The material is introduced into a plate and roller mill, electrically powered by a 250 KW motor, and, since the humidity can reach 14%, the grinding takes place with simultaneous drying through a recovery of the hot gases leaving the rotary kiln. The meal is sucked into an electrostatic filter by a fan driven by a 184 kW electric motor, recovered using augers, and stored in special silos. The vacuum circuit is dedusted thanks to a bag filter. When the mill is stopped, the fume washing tower operates: The atomized water hits the fumes coming from the kiln which precipitate to the ground below forming of moist meal that is collected using augers placed at the base of the tower and then stored in a shed, which will then return to the circulation as a corrective in homogenizing the raw material in the crushing hopper [1].

### 2.1.3 Cooking process

It consists of the semi-wet clinkerisation process carried out in an Ansaldo Smidth-type rotary kiln with cooling satellites, controlled in the kiln head by the firing operator. Raw meal obtained by grinding and taken from the storage silos using augers and bucket elevators is placed in a rotating granulator plate for nodulation with the addition of water. The meal knotted into balls enters the rotating kiln by gravity. The minimum technical flow rate of meal for the kiln in stable conditions is 9 t/h at the inlet while the maximum is 16 t/h. In normal kiln operation, there is a flow rate of inlet meal of 12 t/h. The kiln consists of three cylinders with an internal diameter of 2.85 - 2.40 - 2.70, for a total length of 82 m. It is inclined with a slope of 4% towards the discharge mouth and is supported by four support stations, each equipped with two rollers on which the rolling rings applied to the kiln shell rotates. The combustion process is carried out employing a burner inserted in the exhaust head of the kiln and fed with coal dust which also allows the use of methane gas: the kiln is started with methane gas and subsequently, the coal dust is introduced (the mixture can be petcoke + fossil or simply petcoke, depending on the products available and the relative technical and economical characteristics) [1].

The small balls of meal introduced into the kiln undergo various transformation processes depending on the temperature encountered during the slow-rolling towards the exhaust (the residence time in the kiln is about 4.5 h). The maximum sintering temperature is even at 1450 °C and is reached about 10 m from the exhaust. The meal is then cooked and transformed into clinker, cooled in cylindrical tubes called cooling satellites integrated with the kiln shell, and finally collected on a conveyor with metal drawers for storage. The cooking phase is continuous during the operating period, and this depends on market demands [1].

The clinker is presented in the form of rounded grains with an irregular surface and a diameter of 0.3 to 3 cm. It is essentially composed of CaO, SiO<sub>2</sub>, Al<sub>2</sub>O<sub>3</sub>, and Fe<sub>2</sub>O<sub>3</sub> in various combinations. Its production amounts to approximately 6.5-7.5 t/h. A first check of the clinker is carried out at the exit of the kiln, then it is analyzed in the central laboratory of the plant. This is accumulated and deposited in a covered place waiting for the grinding to produce the cement [1].

The combustion system consists of a horizontal cylindrical ball mill operating with an electric motor, in which the coal is ground and simultaneously dried using the hot air taken from the discharge head of the kiln. This mill, 1.65 m in diameter and 5 m long consists of two chambers [1]:

1. Drying chamber
2. Grinding chamber

The mill is connected directly to the burner installed in the rotary kiln, with a potential of 20,000,000 Kcal/h. The daily coal consumption amounts to about 30 t. The air-coal mixture, through a static separator and a cyclone, is sent into the kiln. By acting on a weigher that feeds the mill, it is possible to vary the flow rate of fuel to be introduced into the kiln. A direct cycle is thus created which represents the simplest and safest solution; the dried coal reduced to a fine powder is not deposited in silos but blown directly into the kiln avoiding stops in the hopper. It takes about a week to bring the kiln cooking system up to speed, while its shutdown takes 24 hours. Atmospheric emissions cease 8 hours after the interruption of operation and are always filtered through pollutant abatement systems. The hot air used in the system is entirely disposed of in the kiln, therefore no dust removal systems are required since no emissions into the

atmosphere are made. The effluents, which derive from the cooking phase in the kiln, can be used in the raw material grinding plant to carry out the drying process of the raw materials. Alternatively, when the grinding plant is not active, they can be sent to an air conditioning and abatement system consisting of a tower and electrostatic filter. In this case, the fumes leaving the kiln (at the average temperature of 350 °C) are sucked into a cooling tower, with a diameter of 3.9 m and a height of 23 m, built in sheet steel, inside the which are installed water sprayers. The operation of the system is controlled by a series of automatic and electronic equipment for regulating the temperature and the water spraying system. The fumes from the kiln, after having treated by water spraying, inside the cooling tower, preliminary conditioning and purification treatment through the elimination of dust particles having larger dimensions, are sucked by an electrostatic filter that filters the emission (through a potential difference induced between the emission and collection electrodes, the separation of the contaminating particles from the gas takes place). A second reserve filter is provided for safety reasons: in case the electro filter does not work due to breakdowns or maintenance, the fumes would be sucked by this secondary filter to guarantee the operational continuity of the kiln [1].

#### **2.1.4 Grinding of terracotta**

The final phase of the production process consists in grinding the clinker with secondary constituents (for example limestone, slag, and pozzolan) to obtain cement suitable for various types of use, as required by the reference standards. The mixture obtained feeds two grinding mills [1]:

- A closed-loop mill with a separator (in a closed-loop process the material discharged from the mill is sent to special centrifugal classifiers that can take the particles of the suitable fineness, while the particles that exceed a certain size are recycled to the mill).
- An open-cycle mill (a more simple procedure that consists in grinding the clinker for a certain time without separating large particles, which therefore remain in the pulverized cement).

#### **2.1.5 Bagging and loading**

The cement taken from the storage silos is sent to an in-line bagging machine and to a rotating bagging unit equipped with an automatic empty bag feeder. The final product is subjected to control in the Central Laboratory and then bagged, loaded, and shipped [1].

#### **2.1.6 Tests and checks**

The cement plant carries out samples of the raw materials coming from the quarry directly in its laboratory. For other raw materials arriving at the plant, instead, reference is made to the written documentation presented by the supplier. Controls are carried out to ensure compliance with legal and internal specifications. The raw materials are stored in suitable places, ready to be included in the production cycle. In case that these materials are identified as a cause of non-compliance with the specifications of the final products, they are removed from the production cycle and subsequently discarded or recovered, and reprocessed to reach the state of conformity. Control plans are foreseen for the products being processed and for the finished products. In case of non-compliance with the specifications, corrective measures are implemented to treat the product adequately and to prevent the phenomenon from happening again. To ensure the compliance required by the UNI EN 197/1: 2007 Standard and by the Decrees of the Ministry of Health dated 10.05.2004 and 17.02.2005, the laboratory carries out checks on the quality of the samples taken from the tanks during the loading phase or from the sales depot bags [1].

## 2.2 Environmental impacts

It is believed that the possible future to keep the kiln alive, necessarily passes from the use of secondary solid fuels (SSF) as an alternative to coal dust. The limited production of clinker, less than 200 t/day, compared to over 2,000 t/day of competitors, does not allow for amortization of costs and competitive prices. The plant has adopted a series of interventions to reduce the environmental impact of the production process. Analyzes are carried out to evaluate the substances present in the various stages of the process. The concentrations of SOX, NO, CO and O<sub>2</sub> are measured continuously in the gas analysis cabin and are checked through graphs in the cabin at the head of the furnace where the firebox operates. The values of CO and O<sub>2</sub> are checked and recorded graphically every hour. An alarm warns the operator when the concentration of O<sub>2</sub> falls below the 1% threshold and when that of CO exceeds 0.5%. If the value of O<sub>2</sub> reaches 0.3% and that of CO to 0.8%, the filter is activated [1].

Working with solid materials that are continuously crushed, ground, and mixed, there is a considerable production of powders that must be controlled and appropriately managed. For this reason, electrostatic filters were installed; an electro filter presented in the mill and activated during the raw grinding phase, and an electro filter presented in the cooling tower. The collection of dust in the silage and bagging points takes place through bag filters. The main device set up for the abatement of pollutants is the cooling tower [1].

### 2.2.1 Cooling tower

The smoke abatement tower from the rotary kiln has a cylindrical steel structure, completely insulated with glass wool panels with 10 cm thickness, covered with aluminum sheets. The central cylindrical body has a diameter of 3.9 and a height of 15 m. Above the upper cone there is another cylinder (2 m in diameter by 5.5 m in height) on which the inlet pipe for hot fumes and dust collected from the kiln is inserted. Below the lower cone, on the other hand, there is a pneumatically controlled valve that allows the discharge of humidified powders, which are removed using a conveyor belt and subsequently collected and reintroduced into the cycle of the raw material. The intake pipe for the cooled fumes is inserted in the lower cone, which must be brought to an electrostatic filter and a bag filter. 21,000 Nm<sup>3</sup>/h of fumes and dust from the rotary kiln enter the cooling tower at a temperature of 360-400 °C exclusively when there is no grinding of the raw material in the mill. As previously described, these effluents undergo the first cooling by expansion and are further treated with water nebulized by the five spray nozzles. These nebulizers are arranged at regular intervals along the circumference of the cylindrical part of the tower. These nozzles are equipped with return nozzles. Each nozzle is equipped with water delivery and return pipes, with a non-return valve on the delivery. The nozzles are powered by a multistage pressure pump, with a 15 cv motor, capable of supplying 0.5-2.5 m<sup>3</sup>/h of water taken from a special tank. The regulation of the flow rate of the nozzles depends on the operating temperature, controlled by an instrument connected to a thermocouple (Fe-Co probe) installed inside the tower. The instrument acts on a special valve that doses the amount of return water, from the nozzles to the storage tank (the higher the temperature, the greater the flow of water introduced into the tower). This treatment determines, in addition to a considerable lowering of temperature, the precipitation of most of the dust contained in the fumes. The residual effluents are then sucked out of the tower at a temperature of about 160-170 °C and directed through an insulated pipe (diameter 0.8 m and length 22.6 m), inside the electrostatic filter thus realizing the dust abatement treatment. The fumes are then emitted from the chimney into the environment at a temperature of 120- 140 °C. The material that comes out

of the electro filter is the raw material of the cement plant, therefore it is recovered and through screws and elevators reaches the storage silos [1].

### 3 Literature Review

Sewage sludge is a mixture of organic and inorganic matter and its composition strongly depends on the treatment and the wastewater origin. It contains various types of pollutants, such as polychlorinated biphenyls, polycyclic aromatic hydrocarbons, dioxins, and heavy metals (Zn, Pb, Cu, Cr, Ni, Cd, Hg, and As). Sewage sludge from municipal WWTPs can follow different disposal routes. In Europe, the most common solution adopted by EU countries is agriculture reuse as fertilizer but, due to several kinds of pollutants contained in the sludge, the reuse on land needs to be carefully monitored to avoid problems for human health and the environment. Sewage sludge landfilling represents another option for disposal, but this solution should be marginal since the European Landfill Directive (99/31/EC) bans sewage sludge landfilling. Mono or co-incineration is another possible alternative especially in those countries where agricultural reuse of sewage sludge is limited or even not allowed [5]. To take advantage of utilizing sewage sludge in mono or co-incineration plants it must be dried since incineration of sewage sludge with high water content in specific grades may not provide any heating value. A general distinction also must be made between partial drying (<85% DM) and full drying (>85% DM). With decreasing water content, the calorific value increases [2]. So the first step can be getting familiar with different modes of thermal drying which are described in the next paragraphs. It is also worth mentioning that the thermal drying phase of sewage sludge is usually done to fully dry the sewage sludge and started having dewatered sewage sludge (70-80% water content) in hands which are obtained by applying different mechanical procedures in WWTPs on sewage sludge (97% water content) and then transported to the thermal drying plants.

#### 3.1 Sewage sludge drying modes

The technological progress, in the drying field, has allowed the development of several techniques that can be divided into three main modes [2]:

1. Convective drying by hot air or hot steam goes through the product with a direct contact causing the evaporation of the product water (e.g., belt dryer, fluidized bed dryer, flash dryer, and rotary dryer).
2. Conductive drying operates by heating the surface of the dryer which delivers the heat to the sludge (e.g., disk dryer, paddle dryer, thin film dryer).
3. Solar drying performing in open or closed tunnel greenhouses.

Table 1 gives an overview of relevant selected dryer designs and typical operating parameters [2].

Table 1 Characteristics and operation parameters of selected driers [2]

	Unit	Dryer type					
		Disc	Thin-film	Drum	Fluidized bed	Belt	Solar
Heat transfer	-		contact	convection, contact	convection, contact	convection	convection, radiation
Medium	-		steam, thermal oil		hot gas, steam, thermal oil	hot gas	solar radiation
Throughput	Mg/a			>2.500		1.000-2.000	200-500
Max. discharge	% DM			>90		50-70	
Energy demand thermal	kWh/kg <sub>water</sub>		0.8-0.85	0.85-1.00	0.8-0.85	0.95	0
Energy demand electrical	kWh/kg <sub>water</sub>		0.05-0.08	0.04-0.12	0.07	0.05-0.08	0.03
Temperature range	°C			85-115		60-70	10-40

Nevertheless, there is a possibility to combine different drying methods and consequently to have hybrid dryers or combined dryers. A more complete comprehension of the drying modes can be obtained by studying the next paragraphs [2].

### **3.1.1 Convective drying**

In convective drying, the drying kinetic starts by a short transient phase also called the adaptation phase. Commonly, we observe an important increase in the evaporation flux until reaching a maximum value and the surface temperature attains the wet-bulb temperature related to the air temperature and humidity. This phase is followed by a second phase also called the constant drying rate phase. During this phase, the evaporation flux remains constant. For the same applied drying conditions, the length of this period is affected by the origin of the sludge. It is also worth mentioning that sludge storage plays an important role in the behavior of the sludge during convective drying, the necessary time to obtain a dry product increases from 300 min to around 600 min when the storage period goes to 20 days. This increase is consequently reflected by a decrease in the drying rate. Also, the results show that while the concentration of VOC decreases with time storage increases, the concentration of ammonia still increases which causes a bad odor. One of the most used driers that are operated on the convection principle is belt driers. Sewage sludge in this drier is dried by (hot) gas, streaming around and through the material, which is transported on a perforated belt. Due to gentle belt transport and gas velocities, an almost dust-free material can be achieved after drying [2].

### **3.1.2 Conductive drying**

In conductive drying with agitators, which represent the almost used conductive drying methods during wastewater sludge treatment there are advantages of [3]:

- No pollution of the heat-carrying medium.
- Steam and odor confinement.
- Low VOC concentration.
- Reduction of fire and explosion risks.

Generally, in conductive drying, mechanical agitation is continuously used to renew the contact between the heated wall and the sludge, which is necessary to keep a high heat transfer coefficient at the heated walls. Nevertheless, during the application of this sort of process, the product passes through three distinguishable phases or zones. Product passes by respectively the pasty phase, lumpy and then the granular phase. These forms are detected by following the variations of the torque with the moisture content decrease. Particular attention is given to the passage of the wastewater sludge by the sticky form (pasty phase), where the performances of the conductive dryer are altered. during the stickiness period, the material deposits on the dryer wall causing the alteration of the hydrodynamics of the dryer, and in extreme cases, it leads to choking the dryer leading to a notable decrease of the dryer performances [3].

### **3.1.3 Solar drying**

In solar drying, the variability of the applied operating conditions that entirely depends on climatic conditions, in particular: solar radiations, temperature, and velocity of the air are reflected in the variation of the drying kinetics. As a consequence, a shorter time drying is registered in summer is obvious. In this method, Sewage sludge is spread over large areas in glasshouses and dried by solar radiation. The humidity is removed by ambient air ventilation. Due to the low temperatures and large air volume streams applied, vapor condensation and treatment is usually not necessary for this process [2]. This process also allows reaching

approximately 70% dry solid content (DSC) without any thermal energy contribution but requires important surfaces (about 700 m<sup>2</sup> for a sludge production of 200 t/yearDM corresponding to WWTP of 10,000 EH). The sludge is frequently mixed for reasons of hygienisation and aeration. Despite its ecological image and low running costs, the market of greenhouse drying is currently limited to WWTP of small size <20,000 EH. The initial investment is significant (about 350–500 €/m<sup>2</sup>) partly because of the civil engineering costs and because of the auxiliary elements (sludge mixing tool and fans) [10].

## **3.2 Sewage sludge innovative drying methods**

Having a look at the sewage sludge innovative drying methods which includes mainly the type of dryers and the heat sources powering the dryer can be helpful since may suit different types of needs for different industries and energy plants.

### **3.2.1 Convective-conductive drying powered by a WTE power plant flue gas**

A suitable integration can be realized between a WWTP (waste-water treatment plant) and a waste-to-energy (WTE) power plant through the recovery of WTE waste heat as an energy source for sewage sludge drying. In particular, sewage sludge thermal drying is performed by collecting the flue gas of a WTE power plant and using it directly without the use of a heat exchanger. Two independent lines constitute the plant, which can treat 600–700 tons per day of MSW (municipal solid waste) depending on the heating value of the materials treated. Focusing on the flue gas treatment line, combustion products exit the economizer at a temperature between 170 and 200 °C. First, they pass in a quencher, which injects nebulized water in the gaseous stream to lower its temperature to 150 C, thus favoring the efficiency of the following processes. After the quencher, sorbalite (a mixture of lime and active carbons) is dispersed into the flow in the throat section of a Venturi. Then, after the bag filter, a wet scrubber and a DeNOx process (Selective Catalytic Reduction –SCR) complete the flue gas cleaning operations [5].

In the process flow diagram (PFD) shown in Figure 2 by integrating flue gas discharge line with wet sewage sludge storage, sewage sludge enters the flue gas pipe directly between the economizer and the quencher. Before the injection, particle size is reduced and made uniform thanks to a milling system. An additional fan (installed in series with the existing WTE fan) performs the dilute phase pneumatic conveying of sludge in the pipe with a loading ratio of around 0.01 kg sludge/kg flue gas (the solid content of the stream is therefore comparable with the dust already contained in the flue gas [5]).

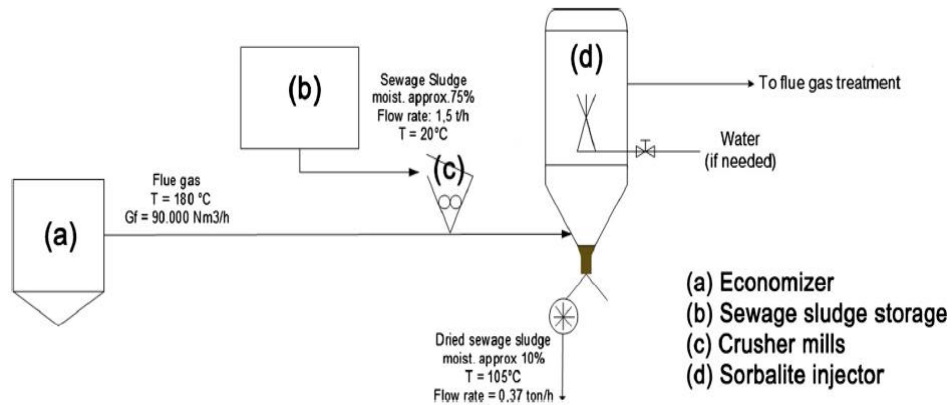


Figure 2 Hybrid convective-conductive drying powered by a WTE power plant flue gas [5]

Finally, the dried sludge is collected from the bottom of the quencher, which has a lower part shaped as a cyclone that separates the dust from the sludge. The process makes it possible of drying 1.5 t/h of wet sewage sludge with approximately 75% water content to the dried sewage sludge with water content less than 10% (with the gas flow rate  $G_f \approx 90,000 \text{ Nm}^3/\text{h}$  and temperature  $T \approx 180 \text{ °C}$ ) [5].

### 3.2.2 Convective-conductive drying powered by a heat pump

In convective belt drying systems air stream with a given temperature and speed passes over the mud to dry the product. To have a more effective hybrid drying system assisted also with conductive heat transfer mode, a heated floor is also added to the process. This hybrid dryer model is coupled to a heat pump model exchanging heat with the air stream using intermediate exchangers. To evaluate the performance of this continuous dryer [14].

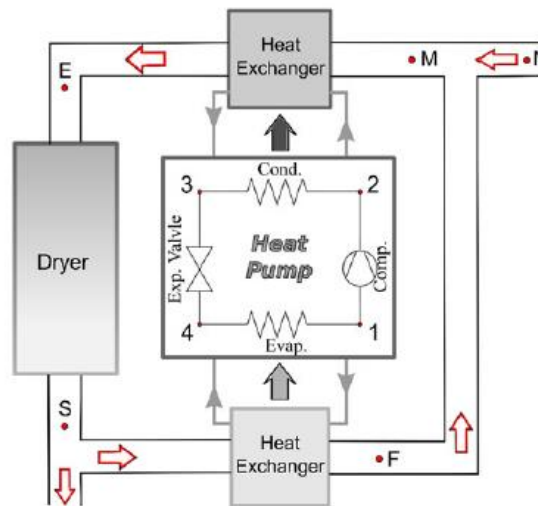


Figure 3 Hybrid convective-conductive drying powered by a heat pump [14]

The upper surface of the pre-dried sewage sludge is exposed to a flow of hot air and its lower surface is heated by direct conduction. The fixed operating conditions at the inlet are air temperature, humidity, and velocity. The temperature at the lower surface of the product is also fixed [14].

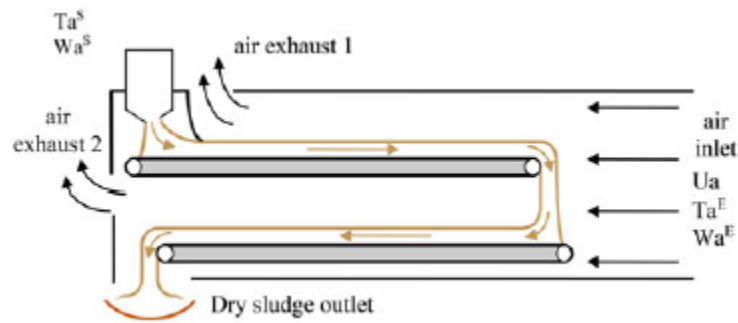


Figure 4 Hybrid drier with two conveyors [14]

The operating parameters of the process like the inlet air temperature and relative humidity are respectively 50 °C and 11% and its velocity is 2 m/s, giving an air flow rate of about 1800 m<sup>3</sup>/h. The temperature at the belt-contacting face of the sample was assumed to be also 50 °C. The sludge introduced in the conveyor is in 30 mm thickness, its initial temperature, and water content are respectively 13 °C and 4 kg<sub>wat</sub>/kg<sub>db</sub>. The dryer is in 2×10 m length, the product crosses this length at a speed of 1.4 cm/min. The air vein is 0.25 m high and 1 m in width. This operating point allows treating 600 kg/day of product. The final moisture content of the product is 0.82 kg<sub>wat</sub>/kg<sub>db</sub>, that is to say, a dryness of 55% [14].

### 3.2.3 Solar-conductive drying powered by a heat pump and solar energy

there is a direct relationship between the sludge surface temperature and the drying rate when referencing solar drying. Hence, to fill in the solar energy for the cold and wet periods, a supplement of energy is needed to reach nearly identical drying performances over a year and to make the greenhouse more compact. To provide the energy supplement, a new drying process which is greenhouse drying assisted by a heat pump can be introduced. This hybrid system combines two energy sources of solar energy and the energy supplied by a heat pump. The heat pump advantage is to offer equal performances all over the year compatible with the needs of WWTP of small and medium-size (from 5000 to approximately 50,000 EH). An even drying rate over the year means a goal of reaching at least a drying rate of 5.5 kg<sub>wat</sub>/day.m<sup>2</sup> (greenhouse drying depends greatly on weather conditions which lead to unequal performances throughout the year e.g. in cold periods a drying rate of 0.5 kg<sub>wat</sub>/day.m<sup>2</sup> is calculated while in summer period it reaches 5.5 kg<sub>wat</sub>/day.m<sup>2</sup>) [10].

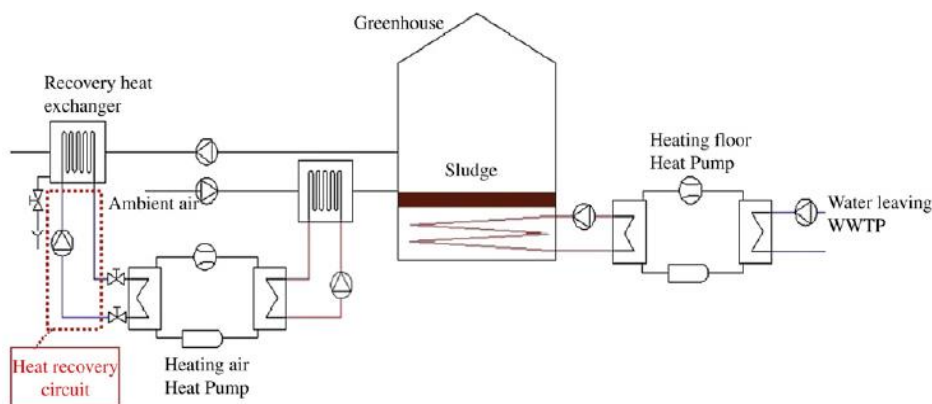


Figure 5 hybrid solar-conductive drying powered by a heat pump and solar energy [10]

The purpose of adding a heat pump is to boost the sludge drying especially in the period of non-favorable climatic conditions. This can be achieved by heating the surrounding ambient air and

hence improving evaporation conditions, and by heating the floor and thus enhancing the diffusive moisture transport from sludge inside to their surface. Therefore, the heat pump condensers transfer their heat to two water circuits: The first water circuit integrated is in the greenhouse floor, and the second one heats the air before entering the greenhouse [10].

The greenhouse floor is made of three layers; the deepest layer is composed of polystyrene panels to reduce the heat losses towards the ground, the second layer consists of a network of polyethylene tubes fixed to the polystyrene panels using studs. The tubes are installed to ensure a uniform flux distribution all over the greenhouse floor. The last layer is made of concrete whose thickness and composition are chosen to handle the various thermal and mechanical stresses; the concrete must tolerate a temperature of 50-60 °C on its surface and approximately 1 t/m<sup>2</sup> of wet sludge. Also, The sludge is frequently (every 12 h) mixed to avoid crusting which limits water evaporation. An automated sludge mixing engine progressively turns upside down the sludge and moves it along the floor [10].

The specific energy consumption at the design point of the heat pump (also considering the solar power) is about 500 Wh for 1 kg of water evaporation (the drying rate at this design condition is about 7 kg/day.m<sup>2</sup>). This amount of energy is an average amount since the obtainable solar power is extremely variable during different months [10].

#### **3.2.4 Convective drying powered by geothermal energy**

This innovative method aims at developing energy-efficient solutions for wastewater and sludge treatment in small islands where geothermal energy is used for sludge drying and it is commonly employed for dehydration of agriculture products that are carried out at lower temperatures [11].

since high temperatures are needed for sludge drying purposes, the geothermal source is employed in a parallel cascade configuration, to produce heat for sludge drying and electrical energy for the WWTP. Part of the electric energy production is used to supply the facilities of a WWTP and the geothermal pumping, whereas the remaining energy is sold to the national grid. Thermal energy is employed to dry the sludge produced within the WWTP [11].

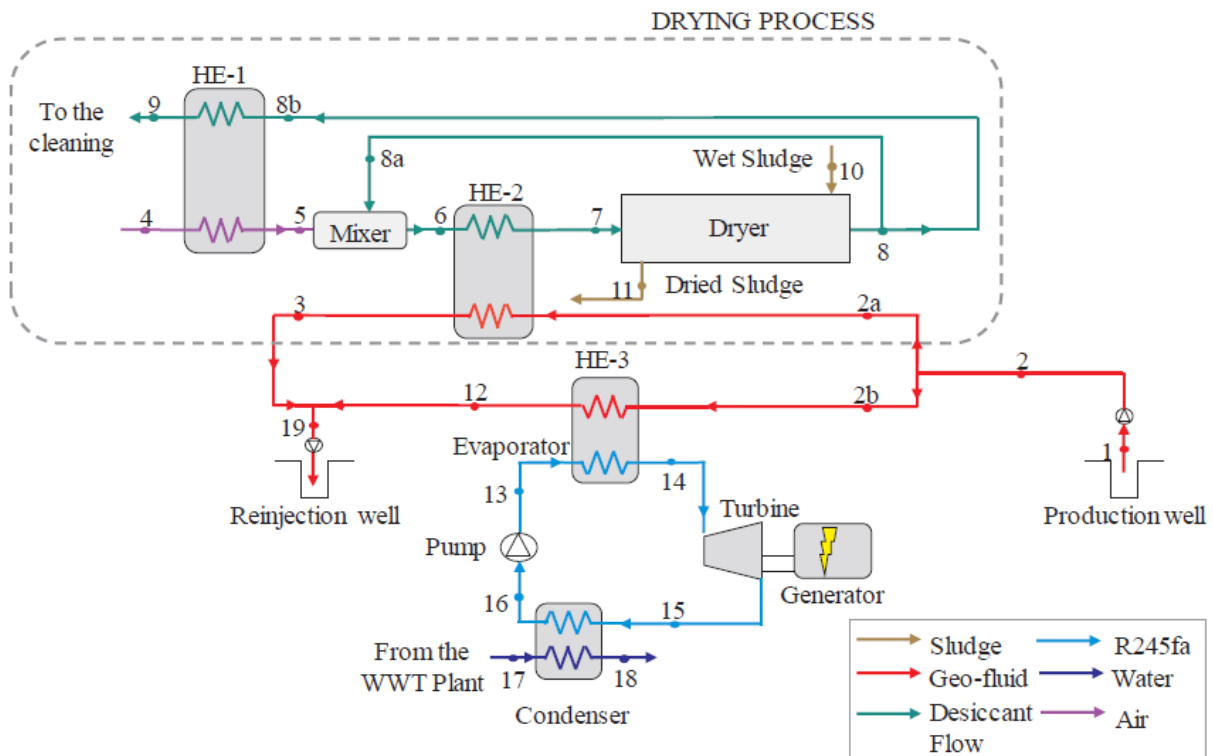


Figure 6 Convective drying powered by geothermal energy [11]

In particular, the geo-fluid coming from the production well is split into two parts; a fraction is used to produce the desiccant flow for the dryer, the rest feeds a small-scale ORC system. The ORC system operates with R245fa, which is a suitable working fluid for temperatures of the heat source up to 170 °C [11].

This system can serve a population equal to 10,000 inhabitants. For sludge treatment, a convective belt dryer, due to easy handling and high flexibility is used. The geo-fluid flow rate in the considered area is estimated to be 5 l/s with a temperature of 140 °C at a depth of 180m from the ground level. The thermal energy required to dry the sewage sludge to a water content lower than 10% and the minimum mass flow rate of geo-fluid needed to supply such thermal energy is calculated and then, the remaining fraction of geo-fluid is used as an input parameter of the ORC unit model. The sludge calorific value calculated equal to 16560 MJ/t<sub>dm</sub> and inlet mass flow rate of wet sludge (75% water content) considered 76.5 kg/h and could be dried to <10% of water content. The proposed system appears to be convenient also from an economic point of view, presenting a simple payback of 5.04 years and a net present value of 1,459,000 € [11].

### 3.2.5 Convective drying powered by CHP units fueled by natural gas

A waste post-process heat recovery unit installment in a medium temperature belt dryer operated in a municipal WWTP with an inlet capacity of 1,830 Kg/h of wet sludge can be a good choice if using a CHP unit. The analyzed sewage sludge drying plant is located within a structure of a municipal sewage treatment plant size 200,000–250,000 p.e. In this plant, sewage sludge management is distinguished by certain phases [6]:

1. anaerobic digestion of sewage sludge in closed digestion chambers
2. dewatering with the use of centrifuges and hygienization process by lime addition
3. drying of dewatered sludge

The dried sewage sludge is sent to a cement plant and combusted in cement kilns. Accordingly, no local low-cost fuel is available for drying purposes and it is required to cover the energy demand by purchasing external fuel (natural gas). Parameters of the sludge which is ordered to dry in a belt drier and a summary of the design parameters of the analyzed belt dryer are presented in Table 2 [6].

Table 2 Main design parameters and performance data of the belt drier [6]

Parameter		Value
Inlet sludge capacity	$\dot{m}_s$	1.83 t/h
Sludge moisture at inlet (after dewatering)	$r_{ws}$	80%
Drying temperature	$t_d$	110 °C
Evaporation rate	$\dot{m}_w$	1.32 t/h
Dried sludge production capacity	$\dot{m}_d$	0.51 t/h
Sludge moisture at outlet	$r_{wd}$	10%
Specific heat consumption	$q_{th}$	1.0 kW h/kg H <sub>2</sub> O
Specific electricity consumption	$q_{el}$	0.085 kW h/kg H <sub>2</sub> O
Heat demand	$\dot{Q}_d$	1300 kW
Electric power demand	$N_{eld}$	110 kW
Post-process air temperature	$t_3$	76 °C
Ambient air mass flow rate	$\dot{m}_{a1}$	3.44 kg/s
Post-process air mass flow rate	$\dot{m}_{a3}$	3.44 kg/s

The maximum design annual capacity of the drying plant reaches 16,000 t of dewatered sludge. Regarding availability factor  $AF = 0.913$  which corresponds to 8000 hours of operation within a year, the annual capacity of the plant is 14,600 t of input sludge and 4,080 t of dried sludge output [6].

The configuration of a heat recovery system is shown in Figure 7. The ambient air (1) needs to be heated to a temperature of about 110 °C to supply the drying process. The required heat is partially generated in three CHP units and transferred by a hot water circuit, and partially is recovered from the post-process air. A reserve gas boiler is also installed in the plant [6].

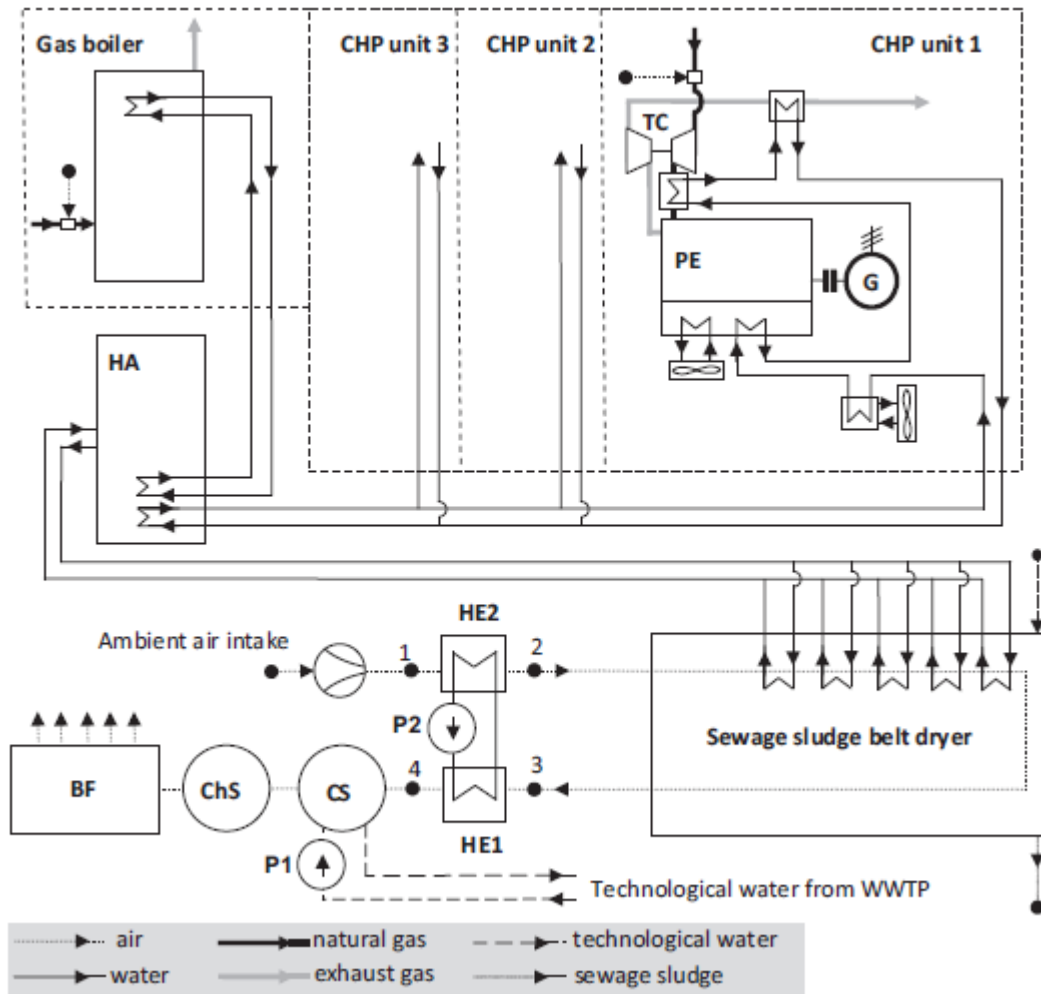


Figure 7 Schematic diagram of a belt drying system assisted by CHP units [6]

Once the enthalpy available in the post-process air is recovered, this air is then supplied to a cleaning system composed of two scrubbers (the cooling scrubber CS and the chemical scrubber ChS) and a biofilter unit BF. For the operation of the biofilter, it is essential to maintain the air temperature below the limit of 45 °C. Heat recovery between the sludge dryer outlet/inlet air is carried out using a water circuit that requires the use of two liquid/gas heat exchangers (HE1 and HE2) and a circulation pump (P1). The drawback of the system is the loss of heat from the constantly operating cooling scrubber CS (the heat is carried away using cooling water) [6].

### 3.2.6 Convective drying powered by a CHP unit fueled by biogas-natural gas

Having considered the convective drying powered by CHP units fueled by natural gas, expecting an effective similar substitution with a CHP unit fueled by biogas besides the natural gas is not that far-fetched. The system is designed considering the capacity and the working conditions of a real plant located in Southern Italy. The layout of the system is sketched in Figure 8 [13].

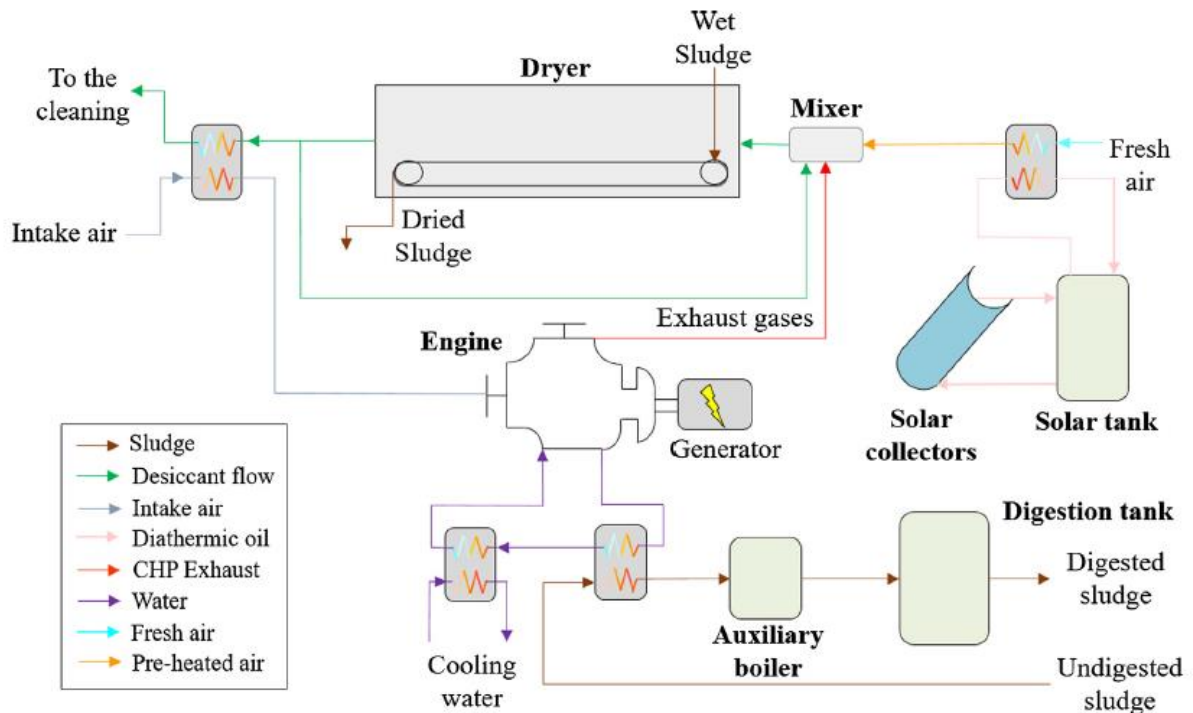


Figure 8 Convective drying powered by a CHP unit fueled by biogas and natural gas [13]

The system aims to ensure a value of dried sewage sludge with a water content of around 10.0%. The drier is designed to treat the average flow rate of dewatered sewage sludge produced in the WWTP, equal to 64.8 t/day, characterized by the average water content of 75.0%. The desiccant current is produced by mixing exhaust gases of the engine, the fresh air, and the recirculated current exiting the dryer. To compensate for the air sent to the cleaning, fresh air is pre-heated through solar energy. The engine size is chosen to fully supply the dryer when solar energy is not available. In this case, the engine operates at maximum capacity, otherwise at partial load. Gases exiting the dryer, that are not recirculated, are used to pre-heat the intake air to the engine to increase its performance. The engine operates with biogas coming from anaerobic digestion of the sewage sludge and natural gas. Low-grade heat recovery of the CHP system is used to sustain anaerobic digestion, which needs thermal energy for a correct operation. An auxiliary natural gas boiler is included to supply anaerobic digestion when CHP heat recovery is not sufficient. The electrical energy produced by the engine is used to supply the entire or a fraction of WWTP demand. When the production is lower than the demand, electrical energy is supplied by the grid. Once there is an excess of production, electrical energy is sold to the grid [13].

### 3.2.7 Convective drying powered by a CHP unit fueled by syngas-WVO

Having considered the two above-mentioned designs, having a CHP unit running just by syngas and waste vegetable oil (WVO) seems a more sustainable solution. The schematic of this design is presented in Figure 9. In this design, wet sewage sludge with a dry solid content of 20-30% (the input flow rate of wet sewage sludge is around 300 kg/h) enters the dryer and is dried up to 90% of dry solids. The dryer exhausts are cleaned by a scrubber and the purified air is discharged into the atmosphere. After drying, the sludge is gasified and the produced syngas is used as fuel in a cogenerative internal combustion engine, together with WVO. The electricity produced by the dual-fuel CHP engine is used for WWTP facilities, while the heat recovered from the CHP cooling system and the exhausts, is used for sludge drying. Low-grade waste heat from the CHP is used to increase WVO temperature or reduce its viscosity and to pre-heat

the fresh air that is mixed with the exhausts. The mixing process is needed to satisfy the thermal requirement of the dryer, in terms of flow rate and temperature [15].

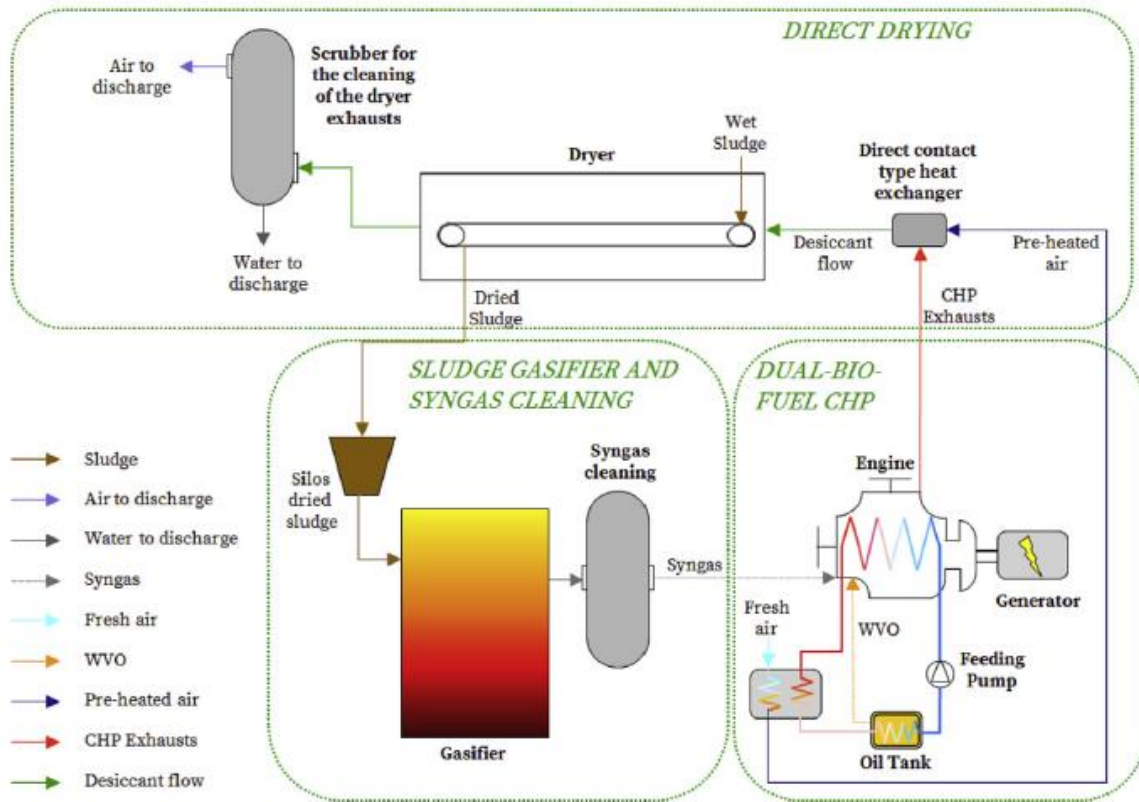


Figure 9 Convective drying powered by a CHP unit fueled by syngas and WVO [15]

In conventional sludge dryers, thermal energy is supplied by a boiler or a CHP system fueled by fossil fuels and/or biogas from anaerobic digestion. Usually, the exhaust gas temperature is in the range of 400-600 °C, while the operating temperature of convective belt dryers is in the range of 120-180 °C. For this reason, intermediary heat exchangers are usually employed for heat exchanging between the exhausts and the desiccant current to obtain the temperature required in the dryer. Instead in this system, a direct contact heat exchanger is considered to produce the desiccant flow at 150-180 °C by mixing the exhaust gas from the CHP system with air pre-heated by low-grade heat from the engine [15].

### 3.3 Sewage sludge drying practices in cement plants

Among dryers, since belt dryers present a design that allows easy manipulation and high flexibility due to the possibility of controlling the process by varying the rate of sludge input to the dryer, the hot air temperature, and residence time by adjusting the belt speed are more in common in cement plants for sewage sludge drying goal [15], even though other methods also are being used for this purposes. Table 3 gives an overview of some of the European cement plants conducting waste heat recovery to dry sewage sludge [19].

Table 3 Dried sewage sludge usage in some cement industries

<b>N</b>	<b>Plant</b>	<b>Company</b>	<b>Country</b>
<b>1</b>	Alicante	Cemex	Spain
<b>2</b>	Allmendingen	Schwenk	Germany
<b>3</b>	Wietersdorf	Wietersdorfer	Austria
<b>4</b>	Wurenlingen	Wurenlingen	Switzerland
<b>5</b>	Huangshi	Huaxin	China
<b>6</b>	Karlstadt	Schwenk	Germany

Sewage sludge thermal drying is not sustainable if the power is fed by primary energy sources, but can be appealing if waste heat, recovered from other processes, is used [5].

#### 3.3.1 Cemex, Alicante

This project was based on the complete integration of a sewage sludge belt dryer within the cement factory of Cemex España in Alicante (Spain). The overall benefits included the use of dried sewage sludge as a substitute fuel in the cement kiln while the quality of the cement is guaranteed, and a reliable end-use for the sludge, as well as energy self-sufficient and 0-odor sludge drying, is achieved [20].

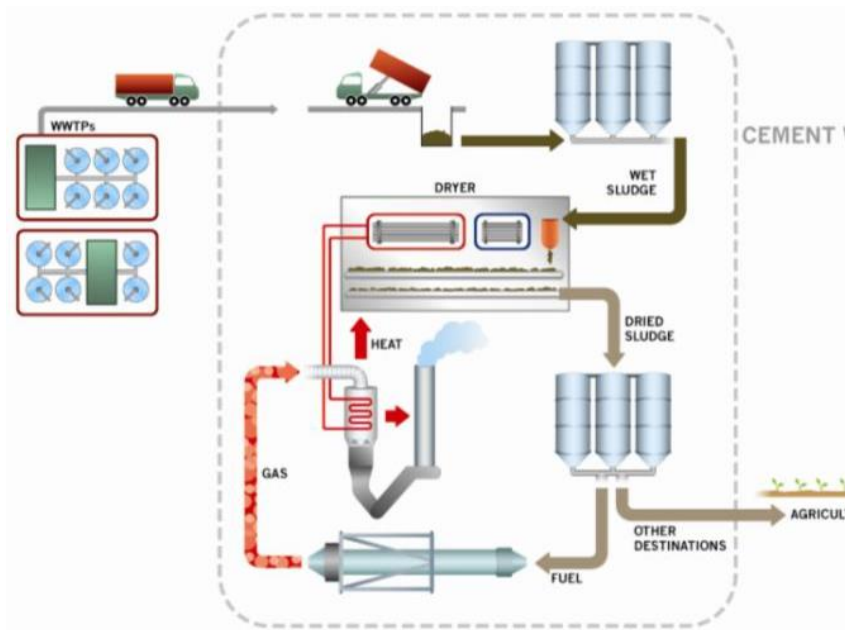


Figure 10 Schematic diagram of the SS management process in Cemex, Alicante [20]

### 3.3.2 Schwenk, Allmendingen

For an economic operation, the drying plant needed to evaporate a minimum of 14 tons of water per hour. Due to space constraints in their existing building, it was impossible to accommodate the two belt drying lines that this evaporation capacity would normally require. Instead, the ANDRITZ DDS 180 which is the largest drum dryer with a diameter of 4.6 m and length of 17 m was installed in the plant to perform sewage sludge drying. The DDS installed in Allmendingen achieves a dry solids content of 90% using only exhaust gas from the cement kiln (about 400 °C) as its heat source [21].

### 3.3.3 Wietersdorfer, Wietersdorf

In addition to the dehumidification of raw materials in an integrated raw mill, the Wietersdorf plant of Wietersdorfer & Peggauer Zementwerke, Austria utilized its kiln line exhaust gas and the cooler mid-air for the drying of blast furnace slag for cement production as well as sewage sludge in separate dryers in 2014. From the data provided by the plant, of the total exhaust gas enthalpy, about 23% is utilized for the drying of raw materials for clinker production and a further 5% for the drying of blast furnace slag for cement production. Another 8% is utilized in a sewage sludge dryer. About 63% leave the process unused as exhaust gases of which 39% could further be utilized. The remaining enthalpy of 24% with a temperature of less than 100°C is considered unusable [19].

### 3.3.4 Würenlingen, Switzerland

This plant uses the waste heat from a cement factory for the drying of dewatered sewage sludge, which then is sold back to the cement factory as an alternative fuel in their clinker production. A similar system is for a cement plant in Karlstadt, Germany, where the entire fuel stream for the clinker production is provided for with the use of alternative fuels. In this case, dried sewage sludge makes up ~10% of the total firing heat capacity [23].

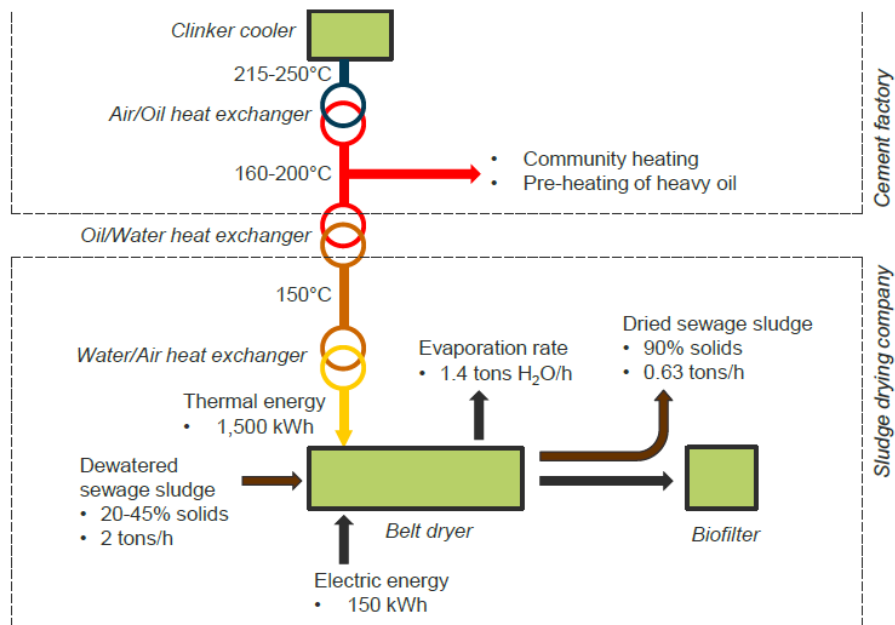


Figure 11 Schematic of SS management process in Würenlingen, Switzerland [23]

### 3.3.5 Huangshi, Huaxin

An industrial practice of SS treatment and co-incineration in Cement Kiln has been done by HUAXIN since 2008. According to the production data, sewage sludge with 50% water content (low heating value) can be easily co-processed in the cement kiln without feeding any additional fuel. Also, Sludge with a water content of about 80% can be fed directly to the cement kiln but will increase the coal consumption in the cement production. It can achieve the harmless disposal of sludge but, cannot realize resource utilization. This cement plant with a waste heat recovery system has a waste heat (<120 C) which is not fully utilized. To utilize this part of heat effectively, Huaxin developed a low-temperature waste heat drying system. Before heat drying, wet sludge from sewage treatment plants is transported to the sewage sludge dewatering plant, discharged to a sludge pit, and then conveyed to a sludge tank through a scraper conveyor. Then the sludge is conveyed to a conditioning tank, followed by the addition of some chemicals to improve the dewatering properties of sludge. After conditioning, the sludge is conveyed to a conditioned sludge tank and stored for filter pressing. At last, the conditioned sludge was pumped to a dedicated sludge filter press which can reduce the water content of sludge to 50%. After all these processes the mud cake was crushed and conveyed to an independently developed preheat device using the low-temperature waste heat from the cement plant and dried to a water content below 50% then conveyed to the calciner via measuring pocket and screw pump and completely be disposed of in the calciner burner [4].

### 3.3.6 Schwenk, Karlstadt

Last but not least, the Schwenk cement factory in Karlstadt presents a more comprehensive documentary on sewage sludge management at their facility. For the manufacturing of cement clinker, a rotating kiln with a daily capacity of 3500 t has been in operation at the Karlstadt cement factory since 1969. The Polysius corporation's kiln system includes a four-stage Dopol preheater, a 90-meter-long kiln, and a Claudius Peters grate cooler (Figure 12). The Karlstadt plant uses 100 percent alternative fuels, with dried sludge accounting for about 10% of the firing heat capacity [22].

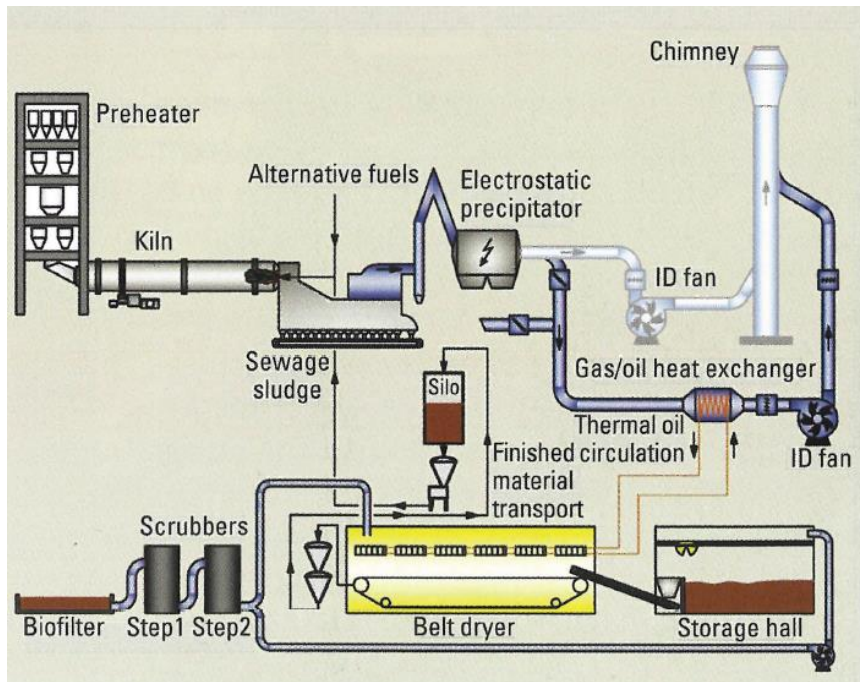


Figure 12 Schematic diagram of SS drying and usage process in Schwenk, Karlstadt [22]

Because the sewage sludge created at WWTP has a water content of 70 to 80 percent, it must be dried further to a water content of less than 10%. The clinker cooler's exhaust air provides 100 percent of the thermal energy required for this purpose. The drying process receives approximately 150,000 m<sup>3</sup>/h of air at 250°C. The cooler exhaust air is chilled from 250 to around 125 degrees Celsius in the process, while the thermal oil utilized as a heat transportation agent to the heat exchangers inside the dryer is heated from 130 to 205 degrees Celsius. In the sludge dryer, an evaporative capacity of around 6.5 MW was predicted to evaporate the water at a rate of 8 t/h. With a heat exchange area of 11500 m<sup>2</sup> and rib spacing of 3.5 mm, the thermal oil heat exchanger is built as a ribbed-pipe heat exchanger. This system is sketched in Figure 13 [22].

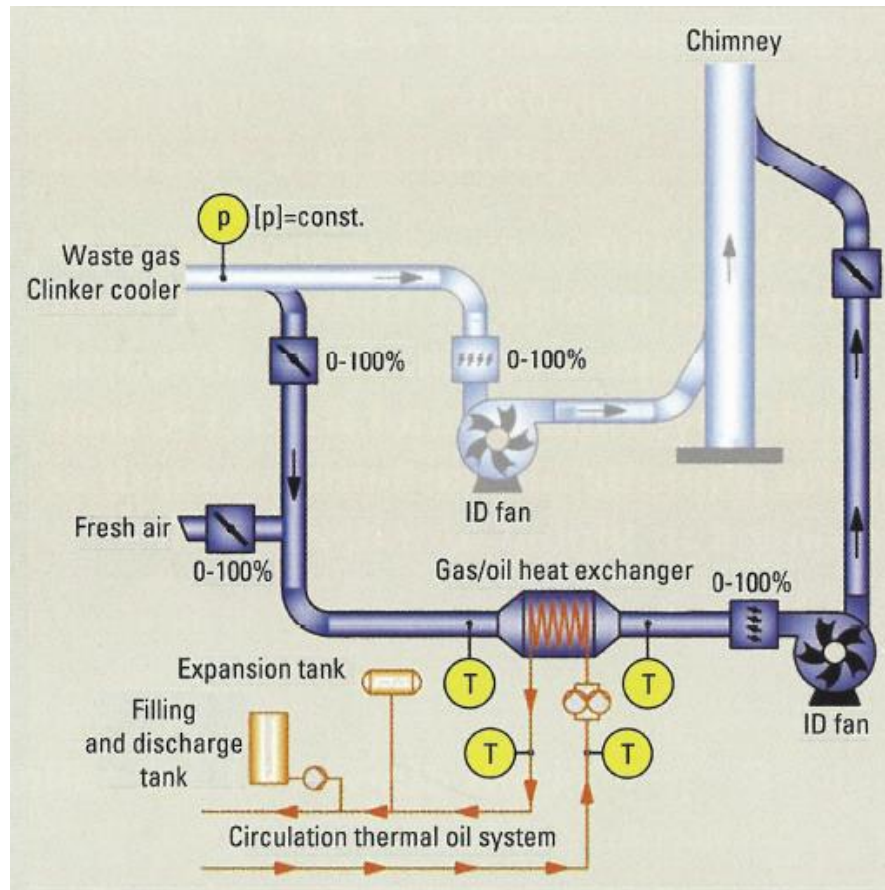


Figure 13 Flowsheet of the waste heat recovery plant in Schwenk, Karlstadt [22]

The drying air is heated with thermal oil/air heat exchangers in the belt drier with a reinforced concrete drying enclosure. The heat exchangers are hot-dip galvanized and have oval steel pipes with smooth ribs spaced at 3.5 mm. The heat exchangers, which are installed on a concrete roof inside the dryer enclosure, have corresponding openings for transporting the drying air. The dryer enclosure has stainless-steel revision doors that provide access to the drying area's interior. The recirculation fans are housed in noise-absorbing panels, and the air ducts are lined with noise insulation to keep noise emissions to a minimum. The dryer's inside is constructed of stainless steel 1.4301, the belt is made of plastic, and the guiding roller is made of stainless steel-plated C-steel. This structure can be viewed in Figure 14 [22].

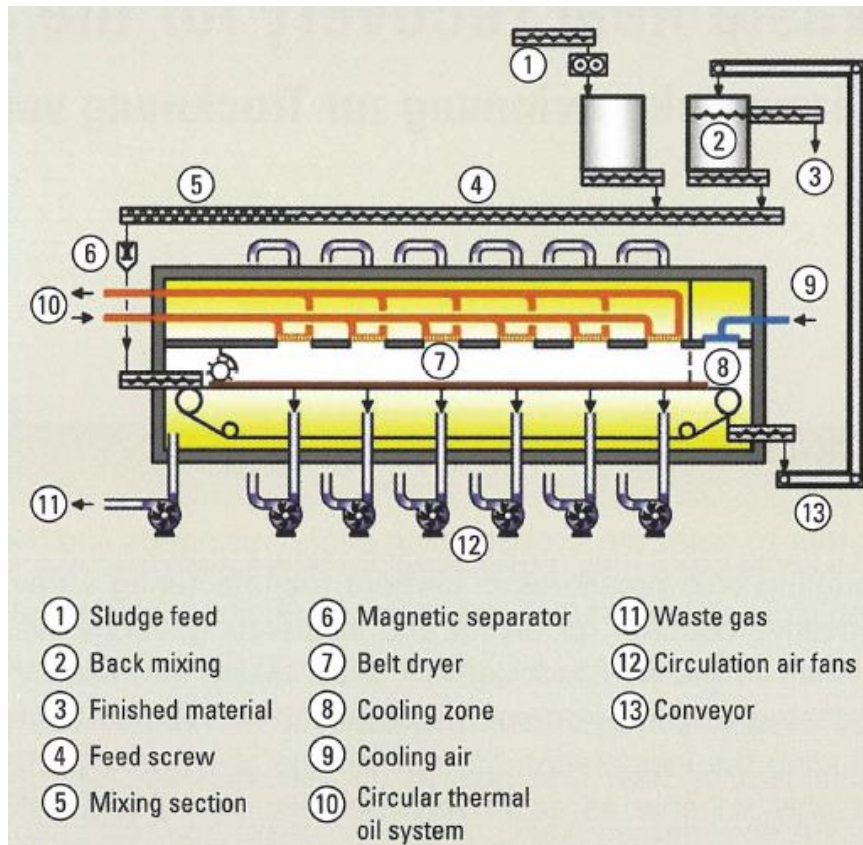


Figure 14 Belt drier design for the sewage sludge drying in Schwenk, Karlstadt [22]

A screw conveyor feeds the input material to be dried, which comprises a minimum of 15% and a maximum of 35% water, via an extraneous material separator and into a collection container. An f-regulated metering screw transports it from there to a feed screw, which is simultaneously fed with a partial feed supply of already dried material. Both ingredients are granulated and combined with around 60% dried stuff using paddles on the feed screw. A magnetic separator is inserted upstream from the feed input to protect the drier from unwanted metallic elements. A distribution screw controls the flow of premixed material onto the belt drier at a steady rate. The distribution reel rotates in the opposite direction as the feed, resulting in a layer thickness of around 60 mm that can be adjusted. The material is penetrated and dried by the pre-heated drying air on the belt. The cooling zone at the end of the belt is flooded with ambient air. The dried material is cooled to 50 degrees Celsius, or a maximum of 30 degrees Celsius above room temperature. The dried material is thrown into the output screw at the end of the belt, and the amount of dry substance is measured by a continuous moisture measurement. The system assures that the dry content of the final material is greater than 90%, depending on fluctuations in the moisture content of the raw material.. A conveyor transports the dried material downstream from the output screw to a combined recirculating mixing/final material container. The processed material is then transferred via a three-layer screening system to a high-pressure pneumatic conveyance system, which transports the final product to a collection silo for rotary kiln firing. The large particles from the screen system are crushed to a size of about 5 mm in a roller crusher with a slotted roller before being added to the finished material. The heat exchangers heat the drying air to a temperature of 125 °C, which is required for the drying process. The heated air circulates across the belt and the layer of material on it, eliminating moisture. The dryer is run at around 5-times the recirculation rate to obtain a high level of thermal efficiency. Six recirculating fans return a considerable amount of the vented

drying air to the heat exchangers, where it is heated to the input temperature. The recirculation fans' speed can be adjusted and is controlled by the pressure difference created by the fluctuating thickness of the material layer on the dryer belt. An exhaust air fan constantly separates some of the recirculated air and feeds it into the exhaust air treatment system. The exhaust air is saturated with water vapor and has a temperature of around 60 degrees Celsius [22].

Treatment of the exhaust air of the drying system and the raw material storage hall is combined by a two-stage chemical scrubber and then fed to a biofilter which is shown in Figure 15. The combination of scrubber and biofilter must reliably meet the standards set by the law (in the case of Germany the agency is TA-Luft) [22].

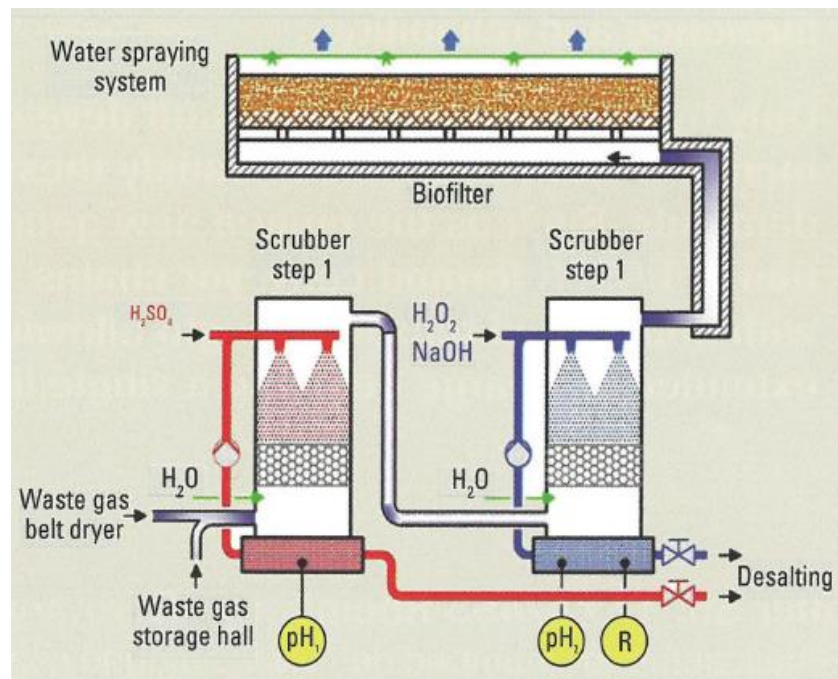


Figure 15 Flowsheet of the chemical scrubber and the biofilter in Schwenk, Karlstadt [22]

### 3.4 Sewage sludge co-firing on cement plants

In countries like Japan, USA, Denmark, Netherlands, Switzerland, and Belgium sewage sludge is used in cement production. In cement production, sludge is usually co-fired with coal in pre-dried form. Pre-dried sludge is easier to store, transport and feed. The sewage sludge for co-combustion is dried (90% DM), pulverized, and pneumatically fed to the burners. Either the sludge is preblended with coal and fed together, or the two fuels can be fed separately if multi-fuel burners are used. The environmental concerns associated with sewage incineration are significantly reduced when sewage sludge is used as fuel in cement kilns. The organic part is destroyed and the inorganic part, including heavy metals, is trapped, and combined in the product [16]. For the same amount of energy, sewage sludge emits 58% fewer emissions than natural gas and 80% less than hard coal and fuel oil. Generally, mono-incineration plants have higher investment costs (between 200 and 400 €/t<sub>dm</sub>) than co-incineration plants (between 150 and 300 €/t<sub>dm</sub>) [24].

For co-incineration of sewage sludge in cement kilns, an upstream full drying (>85% DM) process is usually required, as high-water contents can lead to problems in clinker burning. However, the use of sewage sludge in cement kilns is limited by phosphorus and mercury

content. Phosphorus can impair clinker quality, while mercury is problematic in terms of emissions, due to the absence of flue gas cleaning systems. Also, subsequent phosphorus recovery from the clinker is not possible [2].

In cement production, two traditional positions for fuel firing exists; the calciner burner and the kiln burner [18]. an example of firing in both positions with the results indicating the flame quality will be discovered in the following paragraphs.

### **3.4.1 Sewage sludge firing in the kiln burner**

The purpose of the rotary kiln flame is to provide thermal energy to the raw materials enabling a material temperature increase from ca. 900 to ca. 1450°C to facilitate liquid phase formation and clinkerization reactions. The ideal characteristics of a rotary kiln burner are [18]:

1. To provide a short, narrow, highly radiant flame to enable efficient heat transfer to the clinker bed
2. To ensure full conversion of solid fuels while suspended in the flame
3. To produce a minimum of CO and NO<sub>x</sub>
4. To ensure a stable coating formation in the burning zone
5. To operate with a minimum of primary and transport air
6. To operate with a minimum of excess air
7. To be able to handle a flexible choice of both conventional fossil fuels and alternative fuels

The clinker quality, as well as the stability and efficiency of the pyro system, are dependent on flame qualities. Inefficient heat transfer to the clinker bed can lead to excessive levels of free lime in the clinkers, resulting in decreased alite content and cement strength. A protracted, high-temperature flame may produce undesirable clinker mineral crystal formation, reducing clinker grindability and increasing grinding energy consumption. A too-wide flame can produce impingement on the clinker bed, resulting in increased sulfur evaporation, and flame impingement on the kiln walls can cause coating degradation, reducing the lifetime of kiln refractories exposed to high temperatures. Excessive use of cold primary and transport air might lower the system's energy efficiency. A high excess air ratio may also reduce the energy efficiency and the increased exhaust gas amounts may limit the production capacity [18] , However, In the rotary kiln, it is only possible to observe the flame visually to a limited extent but, some indicators can provide much more information about the quality of the flame than can be obtained from simple visual observation. The most important operation indicators (combustion indicators) with direct relation to firing parameters are [25]:

1. Clinker quality (free lime, liter weight)
2. Burning zone temperature (pyrometer, NO<sub>x</sub>, amps)
3. Coating formation (indicated by kiln shell temperature profile)
4. Exhaust gas composition (CO, O<sub>2</sub>)
5. Kiln inlet temperature
6. Volatilization of circulating elements (hot meal analysis, encrustations in the preheater)

Having some information about the different types of kiln burners can be useful since the main limitations for the quantity of sewage sludge that can be potentially co-incinerated inside the burner and the quality of flame when using sewage sludge is strongly depends on the type of the burner.

### 3.4.1.1 Industrial rotary kiln burners

For clinker production capacities of 1000 to 12,000 t/day, the thermal capacity of the burner in cement kilns with calciners can range from 20 to 250 MW. Non-preheated primary air, which accounts for around 5-15 percent of the stoichiometric air requirements, is normally delivered at a high velocity of 150-250 m/s through the burner pipe. For axial burner momentum and swirling flow, primary air is usually injected both axially and tangentially. Secondary air is provided through the rotary kiln hood from the clinker cooler, which has a temperature of around 1000 degrees Celsius. Excess air ratios of 1.10-1.25 are common. The axial velocity times the mass flow of the primary air normalized with the burner thermal throughput defines the burner momentum of the rotary kiln burner, which can range from 4 to 12 N/MW, with the lowest momentum required for gas firing and the highest momentum required for solid alternative fuel firing. [18].

From the initial generation of mono-channel burners to today's multi-channel burners with a focus on alternate fuel firing, industrial rotary kiln burners have gone through numerous stages of development. The mono-channel burner is a first-generation burner that injects fuel and primary air into the same tube, resulting in a long, slender flame with low radiation intensity. This type of burner is appropriate for wet and semi-wet cement production in long kilns that do not require separate calcination and preheating. High primary air rates are required, and flame characteristics can only be controlled to a limited extent during operation. The multi-channel burners, which were initially created about 1980 to adapt to the shorter kilns introduced by the dry cement process with preheater and separate calciner, are the second generation. Fuel and main air are injected into separate tubular or annular channels. High primary air velocity and often tangential injection result in a short, turbulent, divergent flame, allowing for better control of the flame form and faster mixing with secondary air at reduced primary air consumption. In the late 1980s, the multi-channel low-NOX burner was introduced to meet more strict emission rules. The idea is to separate the flame into fuel-rich and fuel-lean zones by using air staging with two or more injection locations to limit NOX generation during combustion. As a result, the combustion is slowed and the peak temperature is lowered, resulting in less thermal NOX generation. Furthermore, because of the low available oxygen concentration, producing a fuel-rich zone around the burner area reduces fuel-NOX formation. The low primary air amount of this burner type, usually less than 10%, combined with the air staging results in a longer flame length. [18].

Due to the decision that is made by cementi victoria s.r.l. to change their kiln burner, some current examples of burner designs from rotary kiln burner manufacturers are given in this section.

#### **DUOFLEX™ G2 from FLSmidth**

It's a multi-fuel burner that can burn gaseous, liquid, solid fossil, and alternative fuels, or a combination of them. It has central ducts for gaseous, liquid, and alternative fuels inside an annular duct for pulverized coal or petcoke, which is surrounded by a concentric duct with two principal air channels, one for radial air and the other for axial air, which are mixed before being injected via a conical nozzle. The center tube for solid alternative fuels can be straight for fine solids or angled upwards for coarser fuels to modify the trajectory and extend the time the fuel spends in the flame. The goal of the design is to create a simple, reliable burner that is adaptable to operational changes and fuel burning. Figure 16 illustrates this burner [18].

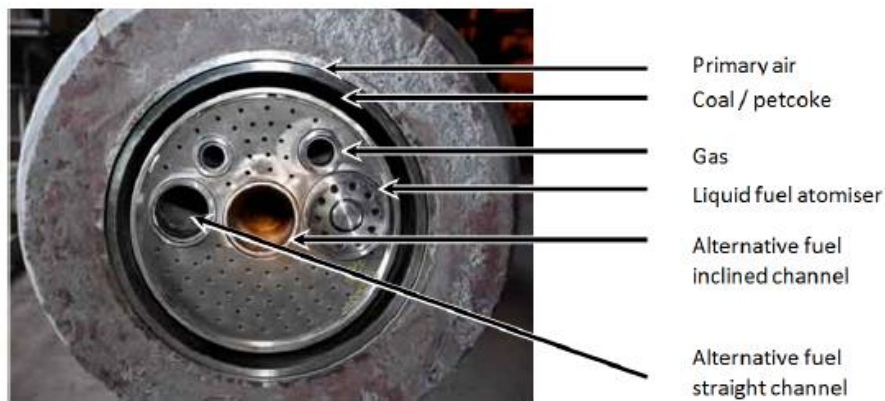


Figure 16 DUOFLEX™ G2 from FLSmidth [18]

### ROTAFLAM®

Figure 17 shows a kiln burner from Pillard Feuerungen GmbH. The axial and swirl air is separated into two concentric channels for pulverized fuel and central tubes for gas, oil, and solid alternative fuels, which are located outside the annular channel. A portion of the swirling primary air is directed into the central alternate fuel channel, which rotates the fuel for better mixing. Primary air usage is typically 8-12 percent of total combustion air, equating to an 8-12 N/MW burner momentum. The goal of the burner design is to create a burner with customizable settings that can handle a variety of operational scenarios and fire as many alternative fuels as possible [18].



Figure 17 ROTAFLAM® [18]

### PYROSTREAM®

The PYROSTREAM® burner is marketed by KHD Humboldt Wedag with the goal of maximizing alternative fuel burning. Outside the coal annular channel, the main swirl air channels, and the solid and liquid fuel nozzles in the middle, the burner contains 12 jet air nozzles. The jet nozzles can be turned 360° to be convergent or divergent to the main spinning primary airflow, and they can be adjusted separately or synchronously. The manufacturer claims that this layout will result in low primary air and burner momentum requirements, with a standard burner momentum of 4.5-5.5 N/MW (not specified if percent of stoichiometric or total air). Figure 18 displays this burner [18].

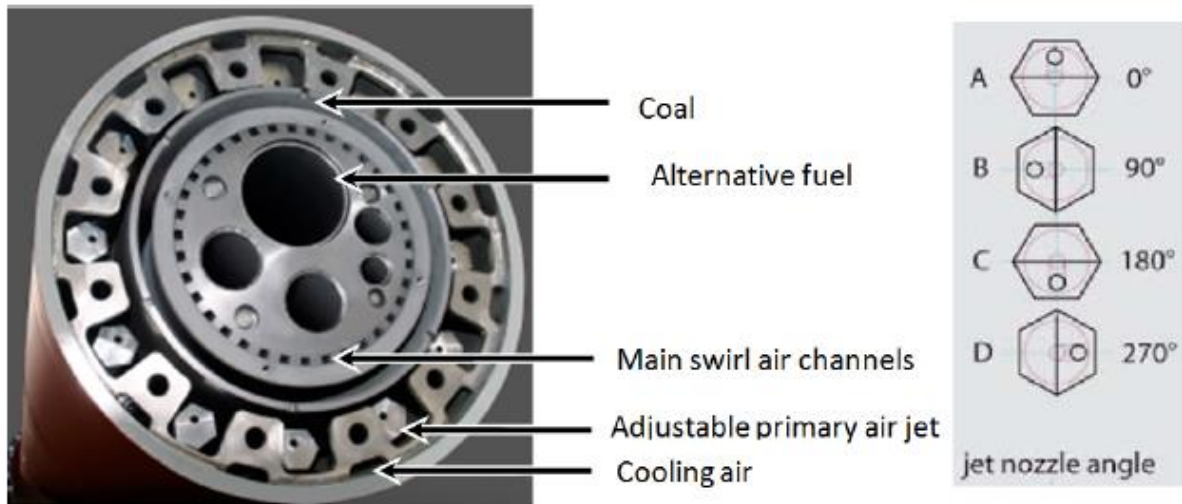


Figure 18 PYROSTREAM® [18]

### POLFLAME®

This burner by Thyssen Krupp Polysius is designed to replace fossil fuels with alternative fuels to a high degree. Multiple primary air jet channels are positioned inside the annular coal channel, around the central fuel tubes. The flame shape and length can be controlled by adjusting the air channels in radial and tangential directions during operation. In the center, solid alternative fuel and liquid fuel tubes are placed. Figure 19 shows this burner [18].

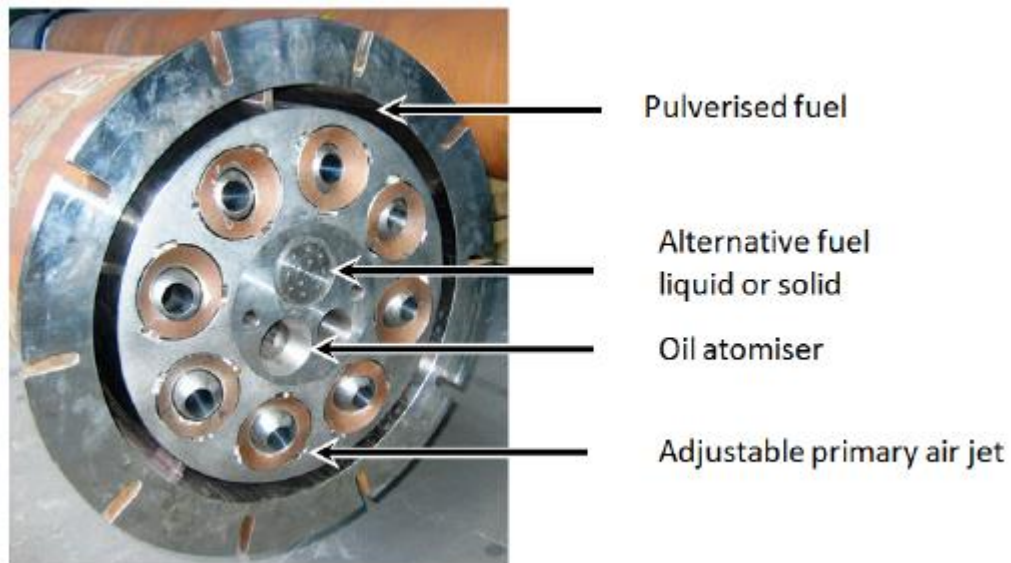


Figure 19 POLFLAME® [18]

### FLEXIFLAME™

This GRECO burner is depicted in Figure 20. This burner has three different primary air injections: external air jets with an axial velocity located at the outer rim, tangential and dispersion air both with an axial and tangential velocity component producing a swirling flow located on each side of the annular coal channel, and tangential and dispersion air both with an axial and tangential velocity component producing a swirling flow located on each side of the annular coal channel. Solid alternative fuel and liquid fuel tubes are positioned in the center.

The amount of primary air is stated as 10-13 percent of stoichiometric air, of which 4-6 percent is external air, and tangential and dispersion air are each 1.5-3 percent of the stoichiometric air amount, with a burner momentum of 6-7.7 N/MW [18].

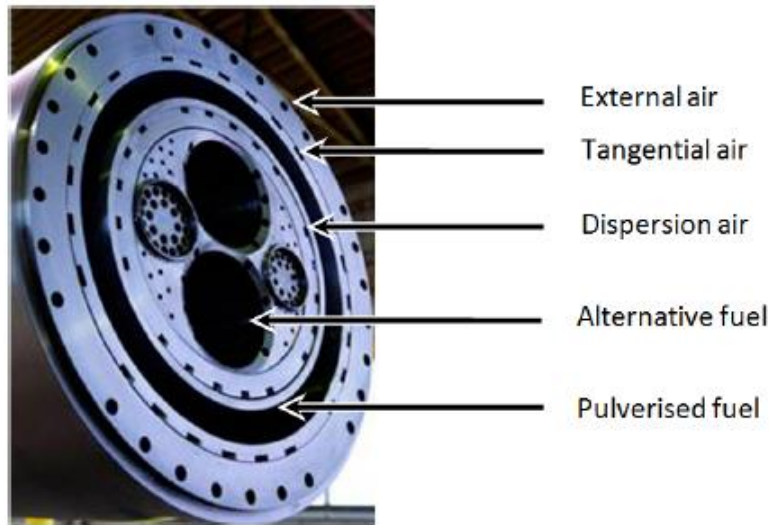


Figure 20 FLEXIFLAME™ [18]

### Mono-Air duct-System

The Unitherm Cemcon M.A.S. burner includes numerous adjustable primary air hoses inserted in an outer annular channel that is used to shape the flame by whirling the entire primary air amount at an adjustable degree dictated by the angle of the air hoses. An extra pneumatic injector system positioned at the circumference of the alternative fuel tube may be used to increase the alternative fuel injection velocity and/or produce a swirling flow to distribute the fuel in the flame zone in the central tube for solid alternative fuels [18].

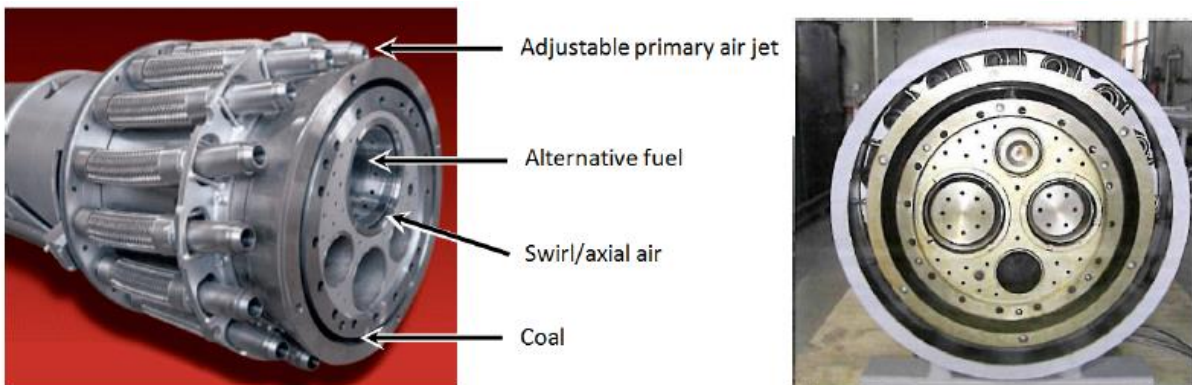


Figure 21 Mono-Air duct-System [18]

### Discussion of burner design

In the previous section, a few modern cement rotary burners were presented. In Table 4 the main design elements of the burners are summarized [18].

Table 4 Industrial rotary kiln burners for cement industry, AF alternative fuels [18]

Burner design	DUOFLEX™G2	ROTAFLAM®	FLEXIFLAME™	PYROSTREAM®	POLFLAME®	M.A.S
Primary air annular channel	x	x				
Primary air jets			x	x	x	x
Separate axial and radial air ducts		x	x	x		
Primary air inside coal					x	
Primary air outside coal	x	x				x
Primary air both sides of coal			x	x		
Annular coal channel	x	x	x	x	x	x
Separate AF central channel	x	x	x	x	x	x
Additional feature of AF pipe	x	x				x

A rotary kiln burner working group led by VDZ in cooperation with the main burner manufacturers started in 2008 to evaluate rotary kiln burners for alternative fuel firing and provide process engineering recommendations of their operation. Based on industrial cement kiln trials of refuse-derived fuel RDF firing with substitution degrees up to 60%, VDZ recommends a minimum axial momentum of 6.5 N/MW and a swirl no. of 0.01 to 0.12 depending on burner type for alternative fuel firing. [18].

Burners for today's cement production must strike a balance between high alternative fuel substitution rates and low NOX generation. Alternative fuels may necessitate greater flame peak temperatures for quick ignition and higher O2 concentrations for faster burnout rates, which could result in more thermal and fuel NOX generation. The principal air injection is the fundamental design parameter that distinguishes commercial burners from one another. The primary air is utilized to shape the flame and control the combustion air mixing pattern. High burner momentum, whirling, or diverging air flows can all affect this [18].

Modern rotary kiln burner designs are increasingly relying on primary air jets, which can be adjusted or locked in position. The primary air jets' purpose is to create a low-pressure zone between them so that hot secondary air can be drawn into the flame zone for better mixing and faster ignition of the fuel. The location of the primary air channel(s) in relation to the annular pulverized fuel channel, whether on the outside or inside, varies by burner design and may result in differences in maximum flame temperature, flame shape, and NOX generation. Burners with primary air on the inside of the fuel channel produce higher peak temperatures near the burner zone, but the temperature downstream of the kiln decays faster. Furthermore, when compared to burners with primary air on the exterior, this burner type produces higher NOX levels at similar swirl numbers. This is thought to be owing to more intensive mixing of pulverized fuel and swirl air, as well as a higher concentration of available oxygen. The flame produced is often wider and shorter than that produced by a burner with primary air on the outside. With increased burner momentum, the difference due to the position of the primary air channel(s) is reduced [18].

The modern kiln burner's fuel flexibility, which allows for a variety of fuel kinds and quality, is a significant design aspect. All of the burner designs exhibited include large diameter central tubular pipes for solid alternative fuel injection to handle lumpy, sticky solid fuel with a significant risk of channel blockage. When compared to injection via the overfire position, the central position of alternative fuel injection has previously been demonstrated to result in superior burnout behavior of the fuel. To avoid pulsating flow and blockages in the alternative fuel pipe, a minimum conveying velocity of 20 m/s is required, with a maximum particle size of approximately 25 mm recommended for efficient pneumatic conveyance to and from the

burner. Significant conveying velocities might cause high wear rates in the tube, which can be problematic. A single symmetrically positioned pipe or multiple asymmetrically oriented pipes can serve as the central alternative fuel channel. With separate feeding of different fuel types, having numerous alternative fuel pipelines increases the burner's fuel flexibility, but at the cost of asymmetric injection into the flame and greater transport air volumes. Alternative fuels that are crushed, dry, and non-sticky, such as dried sewage sludge and animal meat and bone meal, can be handled and injected in the annular channel, which all of the burners reviewed have [18].

Some burner manufacturers have developed new alternate fuel channel injection capabilities. Swirl air can be applied to the fuel channel of the ROTAFLAM and M.A.S. burners to spread out the fuel in the flame. One potential source of concern is the fraction of fuel that gets a downward spin, which could shorten the residence time in the flame and increase the possibility of unburned fuel spilling near the rotary kiln outlet and cooler. The DUOFLEXTM G2 burner allows for the injection of large particle size solid alternative fuel with an upward inclination. Simple trajectory calculations of a spherical particle injected into the center of a 5m diameter kiln with an initial axial velocity of 30 m/s and solely gravitational forces acting on it, resulting in a residence time in suspension of 0.72s and a flight length of 22m. With a 12° upward inclination, the flight time is 1.6 seconds and the flight length is 47 meters, with a maximum height of 4.5 meters. Simple trajectory calculations with axial or inclined injection may give an indication of the available time for combustion in the flame, though frictional drag and the influence of gas fluxes are not taken into account [18].

Getting familiar with different types of burners and their application, it seems useful to bring an example of dried sewage sludge (DSS) co-incineration in a rotary kiln burner. To do so, a practical experience by firing DSS which is provided by [18] is considered. Alternative fuel firing trials in the rotary kiln burner of a modern 5 cyclone preheater, in-line calciner (ILC) cement plant (shown in Figure 22) with a production capacity of ca. 4300 t/d clinker was presented. The original fuel fired in the calciner, and kiln burner is pulverized petcoke. The burner thermal throughput is ca. 60MW and constitutes ca. 40% of the total thermal energy of the pyro-system (the thermal energy is provided by fuel combustion in the calciner constituting ca. 60% of the overall thermal energy input to the pyro-system) [18].

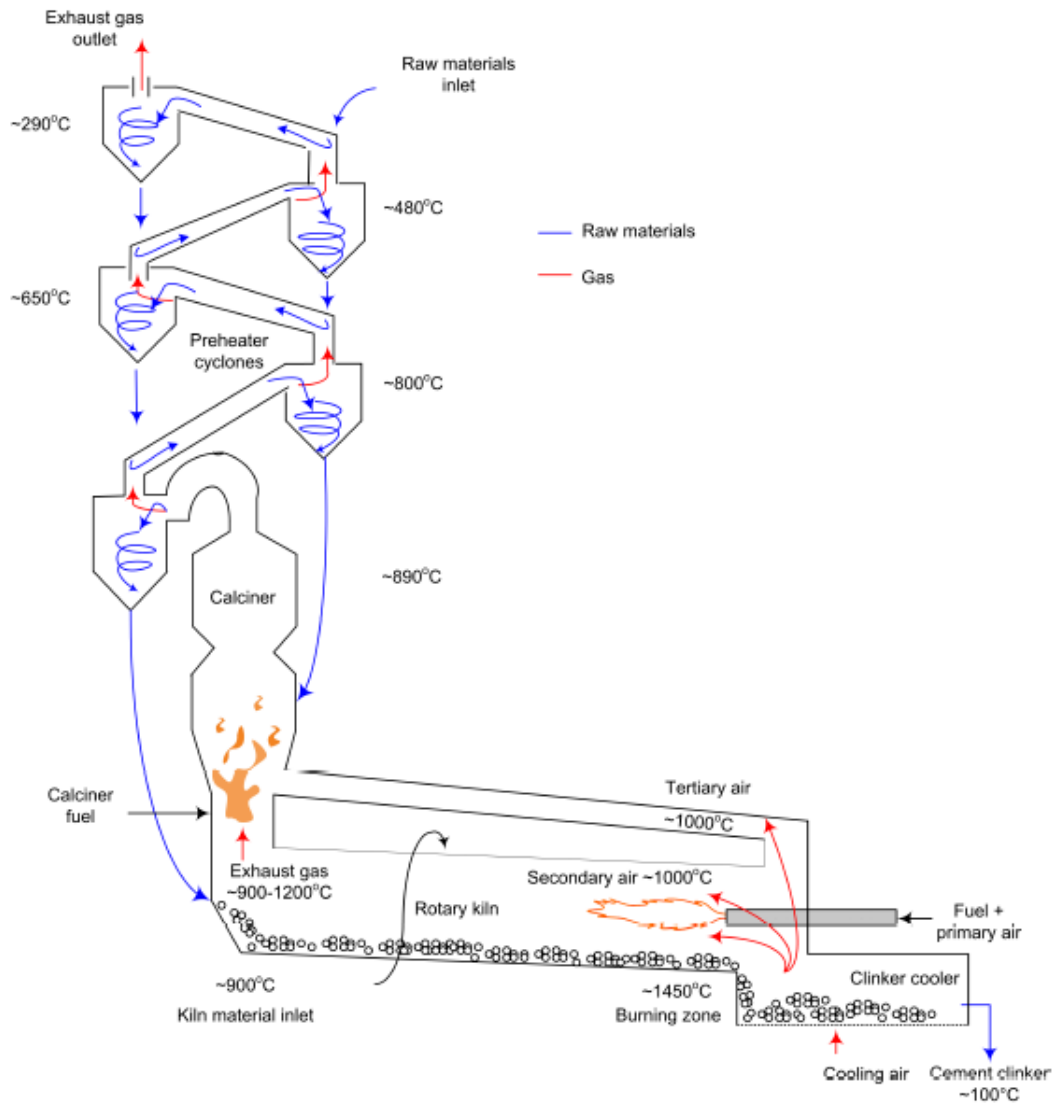


Figure 22 A schematic overview of the in-line separate calciner cement pyro-system [18]

Dried sewage sludge of two qualities, SS B and SS C, were fired in total quantities of up to 3 t/h, corresponding to a thermal input of ca. 13.5 MW. SS B is a pelletized fuel with a cylindrical particle diameter of ca. 4-5 mm and a length up to 25 mm. SS C is a granulated fuel with the main fraction of the particles below 1mm. It is evident that especially SS B will only to a limited degree be converted in the flame and has some consequences. These two types main properties were given in Table 5 [18].

Table 5 Fuel analysis on as received (a.r.) and dry-ash-free (daf) mass basis [18]

Fuel	Moisture [wt% a.r.]	Ash [wt% a.r.]	Volatile [wt% daf]	Char [wt% daf]	Carbon [wt% daf]	Hydrogen [wt% daf]	Nitrogen [wt% daf]	LHV [kJ/kg a.r.]	LHV [kJ/kg daf]
Pine wood	9.3	0.3	85.6	14.4	55.9	7.26	0.04	19.0	21.0
SS A	6.0	18.0	91.2	8.8	56.4	8.16	5.79	17.9	23.6
SS B	8.0	19.9	87.0	13.0	55.2	7.79	7.14	16.5	22.9
SS C	12.2	34.5	90.8	9.19	54.0	7.86	8.26	12.3	23.1

The two cases' main operational conditions were also considered and were given in Table 6.

Table 6 Cement plant operation points during sewage sludge firing trials [18]

Operation conditions	Case 1	Case 2
Clinker production [tpd]	4320	4320
Kiln petcoke firing [tph]	5.4-6.4	5.35
Kiln DSS firing [tph]	0.5-2	2.7-3
DSS mixture mass ratio, [% SS B / % SS C]	60/40	60/ 40 - 50/50
Burner thermal power [MW]	55-66	63-64
Firing ratio kiln [%]	38-45	42
Petcoke substitution, kiln [% of kiln thermal input]	-10 - 6	10-12
Petcoke substitution, total [% of total thermal input]	0-5	4-7
Energy consumption, kiln [MJ/kg clinker]	1.10-1.39	1.26-1.30
Energy consumption, total [MJ/kg clinker]	2.91-3.08	2.97-3.10
O <sub>2</sub> concentration at kiln material inlet [vol%]	2-6	5
DSS injection velocity [m/s]	48.5	30

Case 1 constitutes the initial firing of sewage sludge with a quantity between 0.5-2 t/h and an injection velocity of 48.5 m/s. The O<sub>2</sub> concentration varied between 2 and 6 vol% in the exhaust gas at the kiln material inlet. Case 2 is an optimized operation with 5 vol% O<sub>2</sub> in the exhaust gas and a DSS injection velocity of 30 m/s. These two cases are considered to investigate the influence of DSS firing on kiln shell temperature and sulfur evaporation during DSS firing when two DSS mixtures with different injection velocities are fed into the kiln [18].

#### 3.4.1.2 Influence of DSS firing on kiln shell temperature profile

Two different burner scenarios, approximately 48.5 m/s and 30 m/s, were investigated with regard to DSS fuel injection velocity. At a kiln position of around 30-35 m and 20-25 m with injection velocity of 48.5 m/s and 30 m/s, respectively, trajectory and flame simulations indicate that the SS B pellets will fall out of the flame with only little conversion. In both cases, the particles in suspension have a residence time of around 0.75 seconds [18].

Figures 23, 24, and 25 show kiln shell temperature profiles. In the images, the burner is to the right. Cold regions are created by the placement of 10-12 m and 38-40 m kiln tires for rotation. The kiln shell temperature is shown by color for 0 to 360° kiln circumsphere at the y-axis and kiln length at the x-axis in the top section of the figure. The maximum, minimum, and average values at the kiln circumsphere as a function of kiln length are shown below [18].

Figure 23 displays the kiln shell temperature profile prior to DSS firing. The burning zone, where the clinker bed's liquid phase exists, extends from 0 to 22.5 meters, with a clear and well-defined boundary to the upper transition zone beginning at 22.5 meters. At around 21 m, a single hot spot may be seen [18].

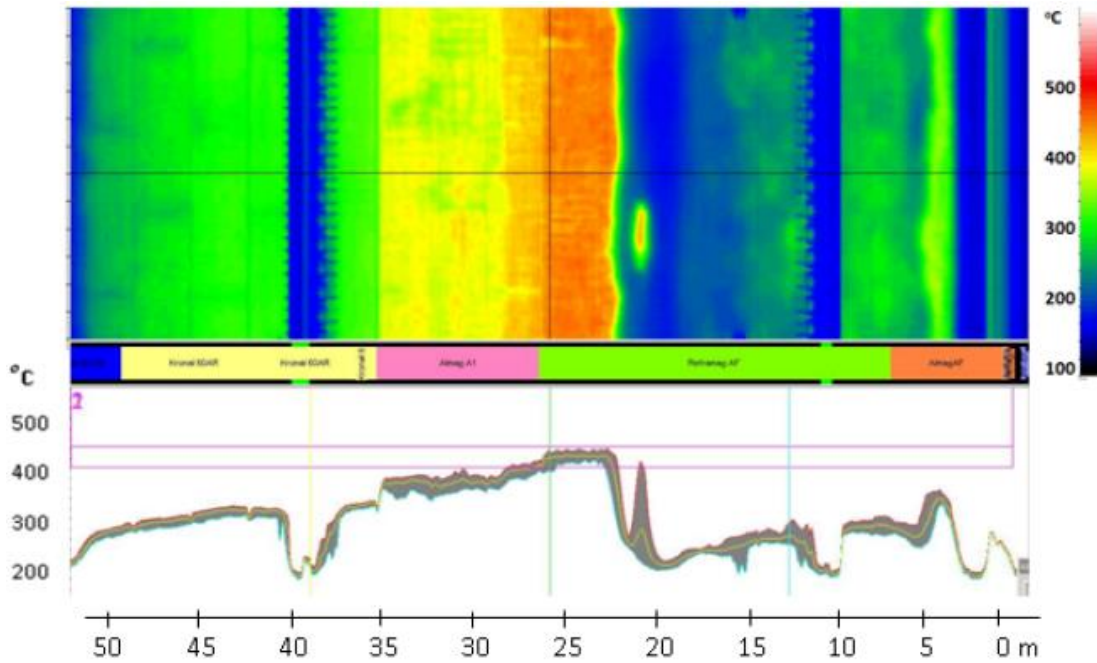


Figure 23 Kiln shell temperature profile before DSS firing [18]

Figure 24 illustrates the temperature profile during a 2 t/h DSS firing with an injection velocity of 48.5 m/s, indicating the creation of a kiln ring in the area of fuel spillage, 30-35 m, and a reduced kiln shell temperature. The formation of a secondary burning zone with partially molten raw materials due to the heat released by the spilled fuel's combustion and/or the formation of a low-temperature melt phase due to reducing conditions caused by direct contact between burning fuel and raw materials may cause the ring to form. If the kiln ring's thickness remains constant, there may be no operating issues. Additionally, due to fuel fallout causing coating defects, the likelihood of hot spots forming in the burning zone has risen during DSS firing. The hotspots' position changes over time [18].

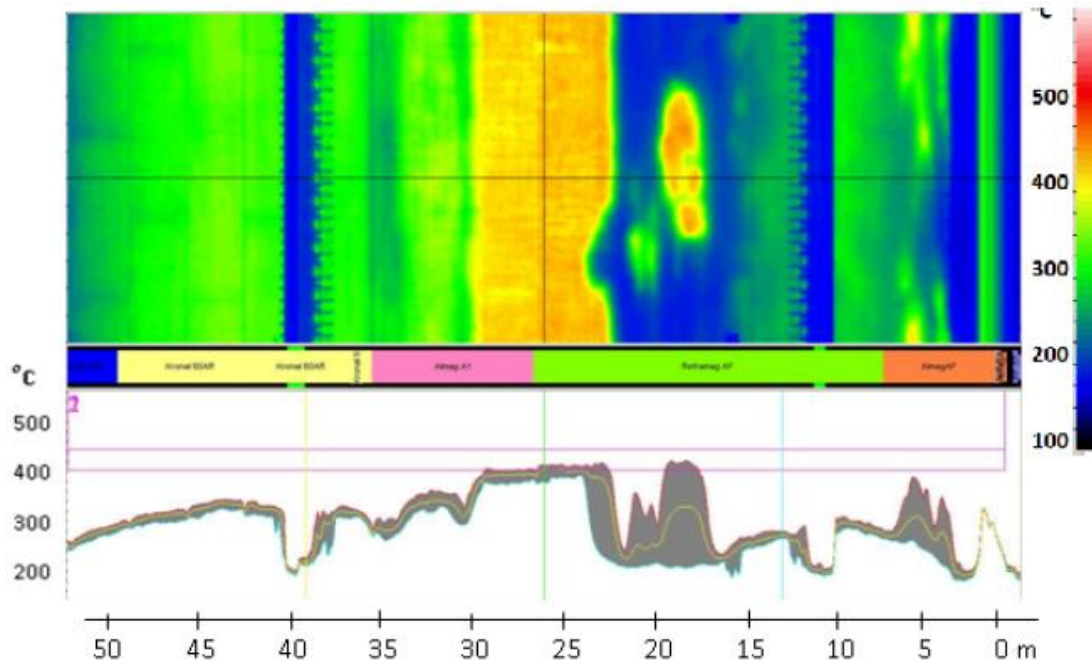


Figure 24 Kiln shell temperature profile with 2 t/h of DSS firing with velocity 48.5 m/s [18]

Figure 25 shows the kiln shell temperature curve during 2.7 t/h DSS burning at 30 m/s injection velocity. In the area between 17.5-21.5 m, where the DSS fuel is predicted to land, a hot zone forms, causing changes in the burning zone coating. In the 30-35 m range, the likelihood of a kiln ring forming is reduced. The DSS firing at any injection velocity has no effect on the length of the burning zone [18].

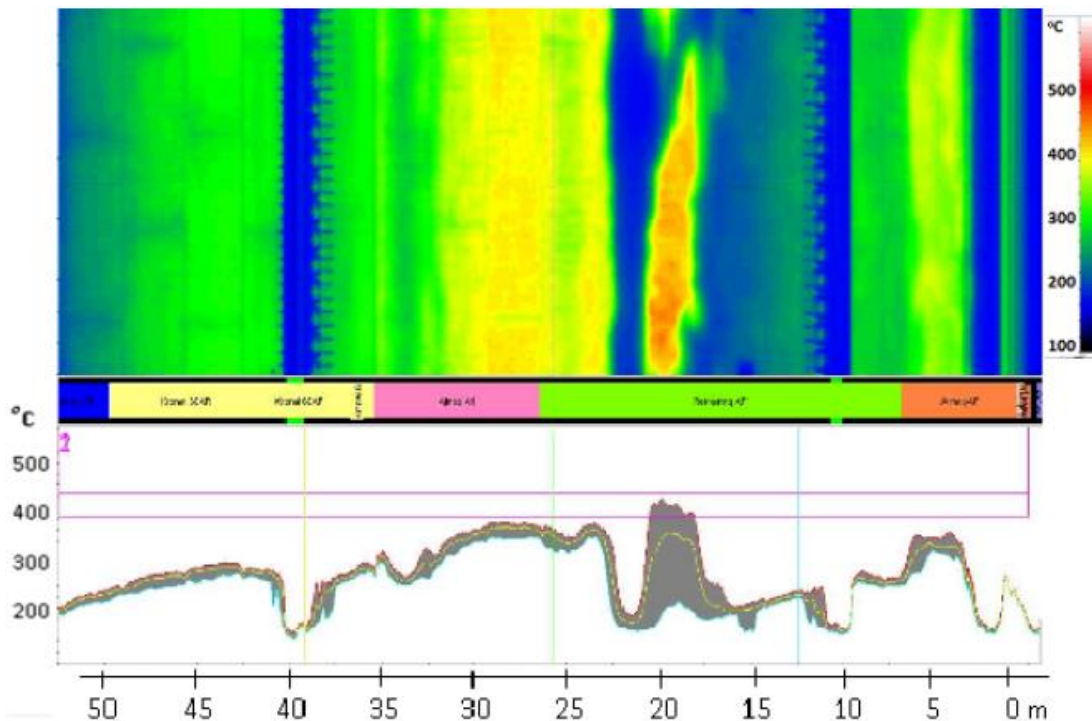


Figure 25 Kiln shell temperature profile with 2.7 t/h of DSS firing with velocity 30 m/s [18]

The preferred DSS fuel landing site, according to the burner experiments, is 15-20 meters from the burner in the burning zone. The DSS energy release may thus contribute to the burning zone temperature, allowing for kiln petcoke substitution and the establishment of a more appropriate

firing ratio between the kiln and calciner. Petcoke substitution was positive in the case of high fuel injection velocity up to 6%, but negative in some circumstances, implying that more petcoke was fired to keep the burning zone temperature constant. Petcoke replacement was between 10% and 12% in the low injection velocity condition. The fuel landing zone could generate a stable hot zone with restricted coating formation, and exterior kiln shell blowers could be used to lower shell temperature if necessary. This is preferable to the more insecure situation of distributed hot spots in the burning zone, which could lead to coating failure. Furthermore, the potential for kiln ring formation at 30-35 m is reduced. In the burning zone, the refractory must be able to tolerate high temperatures and the risk of local decreasing conditions [18].

According to heating values, firing a total of 2.7 t/h of sewage sludge combination with a 60 percent SS B/ 40 percent SS C mass ratio, which is the desired value, corresponds to a 19 percent substitution degree of petcoke in the kiln burner. Due to incomplete burning of the sewage sludge fuel in actual firing trials, petcoke substitution to this level was not achieved, hence the burner's thermal output was raised [18].

#### **3.4.1.3 Sulfur evaporation during DSS firing**

Unburnt fuel from the flame will continue combustion in the kiln bed where local reducing conditions may cause the sulfur release from the raw meal. Before DSS firing the sulfur evaporation factor of the kiln system is 0.25 at ca. 1-2 vol% O<sub>2</sub> in the exhaust gas at the kiln material inlet. This level of sulfur evaporation is acceptable at the cement plant.

Based on findings it is recommended to operate with an O<sub>2</sub> concentration of > 5% at the kiln inlet during DSS firing (0.5-2 t/h) to obtain the same sulfur evaporation factor as before DSS firing. So, a clear correlation is that increased O<sub>2</sub> minimizes sulfur evaporation. [18]

#### **3.4.2 Sewage sludge firing in the calciner burner**

Another industrial practice for sewage sludge drying has been done by Yue Bao cement plant (12,000 t/d clinker production capacity). The dewatered sludge was obtained from the municipal waste-water treatment plants around the Yue Bao cement plant. The water content of this sludge was approximate 78%–83%. Given the high water content and low calorific value of dewatered sludge, the management of the cement plant built a sludge drying plant as well. High-temperature (ca. 300 °C) flue gas from a cement kiln was used to heat the dewatered sludge, and the moisture content in the sludge was reduced from 78% to less than 30% after drying. The dewatered sludge treatment capacity of the plant was 600 t/d and the annual treatment capacity reached 186,000 t. The sludge was pretreated, stirred, and crushed. Meanwhile, the flue gas from the cement kiln was dedusted in a cyclone. The sludge swirled around a spouted dryer, and the dedusted flue gas was utilized to dry the sludge to a water content of below 30% (if the sewage sludge will be dried for a water content lower than 5 % its calorific value reach around 11,000 J/g). The fine-grain dried sludge was collected by a baghouse and then conveyed to a precalciner through a measuring pocket and a screw pump. Finally, the grains were burned in the precalciner [8].

The experiment was conducted on one of these lines. As illustrated in Figure 26 (1. rotary kiln; 2. large volume precalciner; 3. two groups of five-stage cyclone preheater system; 4. OFA pipeline; 5. air pipe; 6. precalciner chamber; 7. coal dust for precalciner; 8. coal dust for kiln; 9. cyclone; A. sludge feed point A; B. sludge feed point B; C. the position of detecting point) the kiln system had three main parts: two groups of five-stage cyclone preheater systems, a

large volume precalciner with a volume of roughly 3,260 m<sup>3</sup>, and a rotary kiln (5.2 m × 70 m). Cement production is a multistage process that involves raw material preparation, preheating, and calcination, as well as clinker burning and cement grinding. First, the raw material is dried by the hot exit gases from the precalciner and the rotary kiln. Part of the carbonate is decomposed in this stage. Then, the dry raw material is calcined and decomposed in the precalciner, which is located between the rotary kiln and the preheater section. The calcination process can almost be completed (>90%) before the raw material enters the rotary kiln when 60% of the total fuel (coal) of the kiln system is added to a secondary combustion chamber that is installed in the precalciner. The process begins by decomposing CaCO<sub>3</sub> at roughly 900 °C to retain CaO and CO<sub>2</sub>. In the subsequent clinker burning process inside the rotary kiln, oxidizing conditions and a maximum material temperature of 1450 °C must be maintained to facilitate the required sintering reactions. Finally, the clinker is obtained, cooled, and then ground together with gypsum (approximately 5%) and other materials to produce cement. The flow type between the gas and solid phases is countercurrent in the production process. In the production process, the dried sludge provided 3%–10% (assume 10 % corresponds to a feed rate of 9 t/h of dried sewage sludge) of alternative energy and was fed to the precalciner [8].

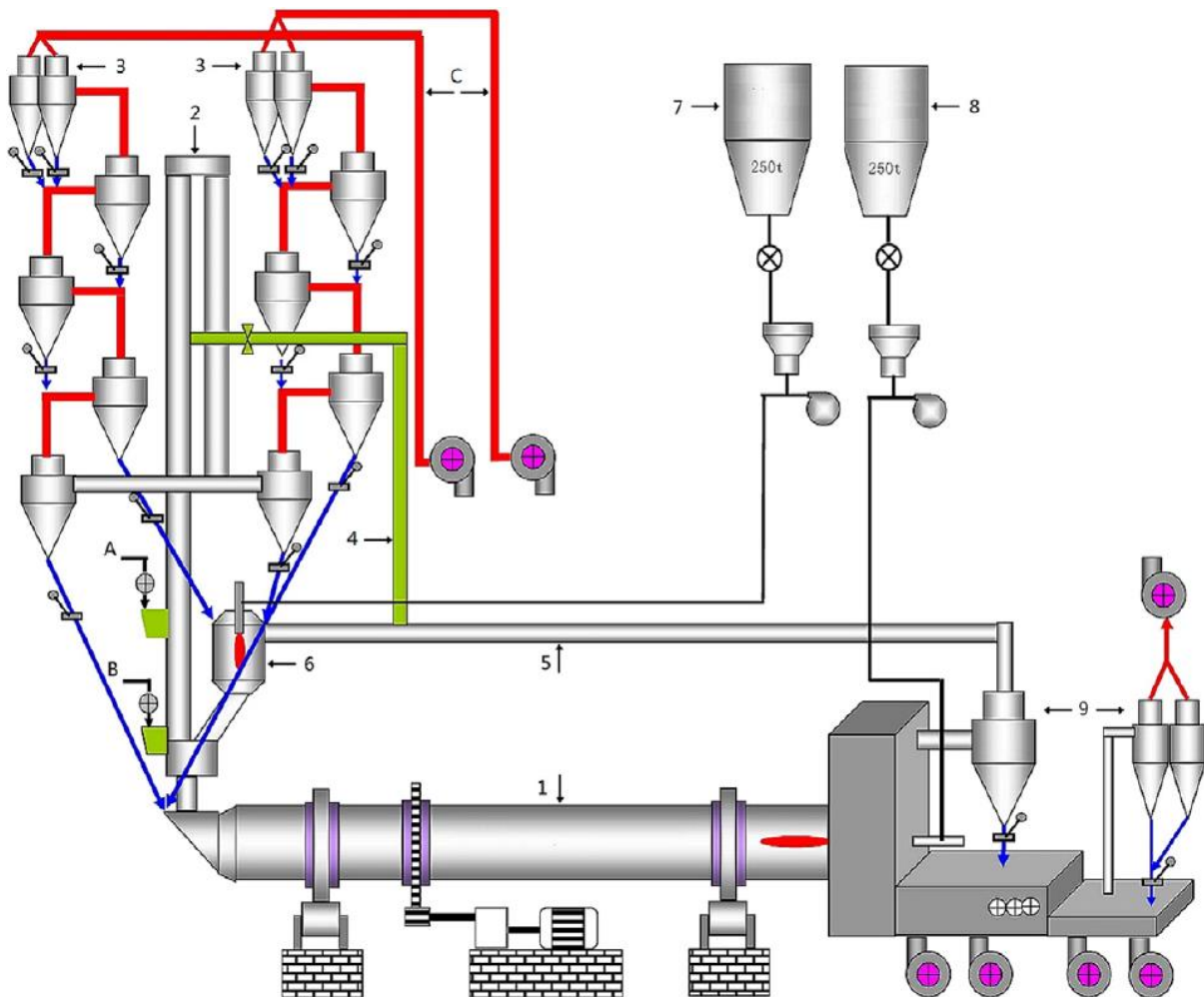


Figure 26 Schematic presentation of the cement manufacturing process [8]

As shown in Figure 26 there are two sludge feed points in the precalciner. Point A was in the re-burning zone, in which the temperature was roughly 850 °C-1000 °C. Point B was in the primary combustion zone, where the temperature was approximately 1000 °C-1100 °C. In this study, a sequence of experiments was conducted to evaluate the influences of different

operational parameters on NOX removal. Specifically, the influences of feed rate and feed point were investigated systematically. The system stability must be maintained for at least 1 h when the operating condition changes. Concentrations of pollutants (NO, CO, and O<sub>2</sub>) were monitored continuously using a flue gas analyzer (testo350XL, Germany) for 2 h. As Figure 26 displays, the detection point was located on the flue gas outlet pipe of the five-stage cyclone preheater system [8].

The analysis results indicate that the use of sewage sludge as an alternative fuel for cement clinker manufacture is technically viable. NOX removal of this technology can be more than 65%, and the use of sludge as alternative fuel does not affect cement clinker quality negatively (Table 7, 8) [8]. The study does not refer to up to which quantity of sewage sludge usage, the cement quality remains unchanged but it can be assumed that it refers to a usage of 9 t/h of dried sewage sludge as an alternative fuel [8].

Table 7 The chemical composition (wt.%) of cement produced with and without SS as fuel [8]

Sample	SiO <sub>2</sub>	Al <sub>2</sub> O <sub>3</sub>	Fe <sub>2</sub> O <sub>3</sub>	CaO	MgO	f-CaO	R <sub>2</sub> O	SO <sub>3</sub>	LOI	Cl <sup>-</sup>
With sludge	21.20	5.29	3.73	65.57	1.35	1.02	0.48	0.90	0.08	0.020
Without sludge	21.23	5.35	3.86	65.67	1.01	1.01	0.52	0.92	0.09	0.018

Table 8 The mineral composition (wt.%) of cement produced with and without SS as fuel [8]

Mineral composition (wt.%)			
C <sub>3</sub> S	C <sub>2</sub> S	C <sub>3</sub> A	C <sub>4</sub> AF
58.23	16.93	7.71	11.33
57.76	17.38	7.66	11.73

The results indicate that sludge feed point (Table 9) and sludge feed rate (Table 10, 11, 12) and significantly influence NOX reduction, CH<sub>4</sub>, HCN, and NH<sub>3</sub> are the key species for NOX reduction. The technology can offer an attractive approach for controlling NOX emission from the cement industry and disposing of sewage sludge safely [8].

Table 9 The effect of feed point on NO<sub>x</sub>, CO, and O<sub>2</sub> emission at the feed rate of 9 t/h [8]

Feed point	CO (mg·m <sup>-3</sup> )	NO <sub>x</sub> (mg·m <sup>-3</sup> )	O <sub>2</sub> (vol.%)
No sludge addition	359.45	516.55	0.65
Feed A	273.94	166.34	0.12
Feed B	301.92	387.94	0.66

Table 10 Feed rate of dried sludge in the different series [8]

Series	Feed rate (t·h <sup>-1</sup> )	Series	Feed rate (t·h <sup>-1</sup> )
Series 1 (S-1)	A-0, B-0	Series 2 (S-2)	A-0, B-9
Series 3 (S-3)	A-3, B-6	Series 4 (S-4)	A-4.5, B-4.5
Series 5 (S-5)	A-6, B-3	Series 6 (S-6)	A-9, B-0

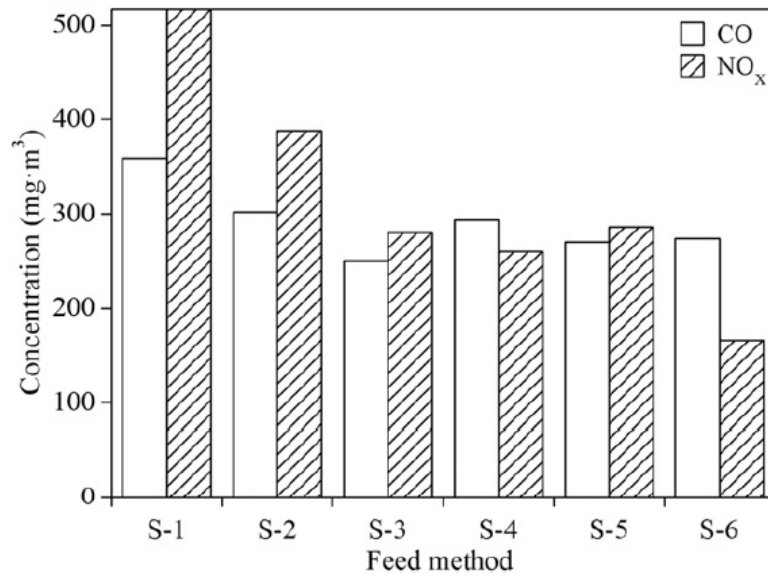


Figure 27 The effect of the sludge feed method on NO<sub>x</sub> and CO emission [8]

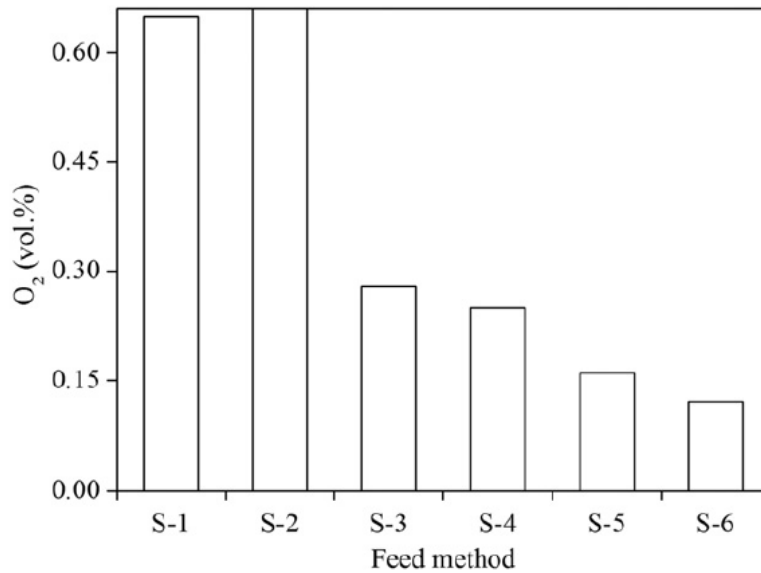


Figure 28 The effect of the sludge feed method on O<sub>2</sub> emission [8]

### 3.5 Eco-cement quality when DSS added to raw materials

The effects of using dried sewage sludge as an additive on cement property show that if the eco-cement samples were prepared by adding 0.50 to 15.0% of dried sewage sludge to unit raw meal, and then the mixtures were burned at 1450 °C for 2 h in the experimental condition, the results indicated that the major components in the eco-cement clinkers were similar to those in ordinary Portland cement. In particular, the eco-cement raw meals were prepared by mixing various amounts of dried sewage sludge per 100 kg dried raw meal, and the resulting types of eco-cement raw meals contained sewage sludge at 0, 0.50, 1.0, 1.5, 2.0, 2.5, 3.0, 5.0, 8.0, 10.0, 12.0 and 15.0 %, respectively (by weight of raw meal). All the grounded raw mixtures were burned in a programmable electrically heated furnace to form eco-cement clinkers. The high-temperature furnace temperature was raised by 6 °C/min from room temperature and maintained at 1,450 °C for 2 h (the total process required 8 h). After burning, the resulting products were cooled rapidly in the air. All the eco-cement clinkers were pulverized and thoroughly ground in a ball mill until most of them could pass through a #200 mesh (with 75

$\mu\text{m}$  pore diameter) metallic sieve (retention on the mesh sieve was less than 5% in weight). Finally, a sample of each eco-cement clinker was co-ground with 5% and 15% per weight of gypsum and fly ash to produce the corresponding eco-cement. The mortar mixtures of twelve eco-cement samples were prepared according to GB/T 17671-1999 (the standard test method for the strength of hydraulic cement mortar in China). The ratio of sand/eco-cement (by weight) was 3:1, while the water to eco-cement ratio was fixed at 0.50. Mortars were put in  $40\times 40\times 160$  mm molds to obtain specimens and were stored in a moisture room at  $20 \pm 1$  C for 24 h. Afterward, all the specimens were de-molded and cured in a water bath with a steady temperature of  $20 \pm 1$  C for 3 to 28 days. Finally, the flexural strength and compressive strength development of the specimens were measured at the curing ages of 3, 7, and 28 days. Chemical and physical analyses of the eco-cement clinkers, ordinary Portland cement, and eco-cement pastes were conducted in terms of particle distribution test, flexural strength and compressive strength test, setting time, heavy metal leachability, heavy metal concentration, chemical composition, mineralogy, and SEM. The results show that the size distributions of both the raw meals and eco-cement clinkers met the industrial quality criteria for cement. Also, the X-ray diffraction (XRD) pattern results for the plain clinker and the eleven eco-cement clinkers indicated that the major components of the eco-cement clinkers were  $\text{C}_3\text{S}$  [ $\text{Ca}_3\text{SiO}_5$  and  $\text{Ca}_3(\text{SiO}_4)\text{O}$ ],  $\text{C}_2\text{S}$  ( $\text{Ca}_2\text{SiO}_4$ ),  $\text{C}_3\text{A}$  [ $\text{Ca}_3\text{Al}_2\text{O}_6$  and  $\text{Ca}_3(\text{Al, Fe})_2\text{O}_6$ ],  $\text{C}_4\text{AF}$  ( $\text{Ca}_4\text{Fe}_2\text{Al}_2\text{O}_{10}$ ) and all were similar to those of ordinary Portland cement. Moreover, the phase formation of  $\text{Ca}_{54}\text{MgAl}_2\text{Si}_{16}\text{O}_{90}$  was identified in all the clinkers. However, the  $\text{C}_2\text{S}$  ( $\alpha\text{-C}_2\text{S}$  or  $\beta\text{-C}_2\text{S}$ ) phase formation increased with the increases in sewage sludge content. The XRD phase identification study also demonstrated that the increase in  $\text{C}_2\text{S}$  was not obvious until the sewage sludge content exceeded 10% (per raw meal by weight), and it was easily seen to be higher at 12 and 15%. In addition, some phase formations containing heavy metals (Cr, Zn, Ni, Cu, et al.) could also be found when the sewage sludge content was greater than 5%. In general, the general trend was that  $\text{C}_2\text{S}$  and components with heavy metals increased with increases in sewage sludge content in the raw meal. Also, in comparison with the plain paste, the results demonstrate that the flexural and compressive strengths of eco-cement paste were similar under the same curing age conditions. Also, the results show that the addition of sewage sludge into a raw meal can potentially cause delayed hydration of the clinker pastes especially when the dried sludge contents go higher than 10% concerning when the content is below 10%. Moreover, Al and Fe, known to be the main compounds of cement, decreased slightly as the sewage sludge content in the raw meal increased. However, studies have shown that properly increasing the amount of aluminum oxide in clinker can enhance early hydration and increase the early strength of the pastes [7].

The analysis results of an actual project indicate that the use of sewage sludge as a denitration agent and alternative fuel for cement clinker manufacture is technically viable. NOX removal of this technology can be more than 65%, and the use of sludge as alternative fuel does not affect cement clinker quality negatively [8].

### **3.6 Eco-cement quality when DSS Ash added to raw materials**

Using SSA (sewage sludge ash), as a mineral component, has a negative impact on almost all mortar or concrete materials parameters. The activity of SSA in cement-based products depends mainly on its oxide and mineralogical composition as well as the type of used binder. The deterioration of mechanical properties is observed when low-active SSA even in small amounts

is used. However, the negative impact of the presence of SSA on cement mixtures can be reduced by modifying the ratio of active oxides [9].

### **3.7 Flue gas treatment**

If waste is used in cement kilns, often emissions of TOC and mercury, especially in the case of using sewage sludge, are monitored from the exhaust gas of cement kilns (in some cases continuously), additionally to the regular continuous measurements of dust, NO<sub>x</sub>, SO<sub>2</sub> and CO emissions, which are carried out. Depending on the input and the types of waste fuels used, process conditions, and the relevance of the emissions, additional measurements are carried out for HCl, HF, heavy metals, benzo-a-pyrene, benzene, and polychlorinated dibenzo-p dioxins (PCDD), and polychlorinated dibenzofurans (PCDF). Furthermore, for the use of waste often recurrent measurements are carried out, e.g. once a year [17].

## 4 Case study

Regarding the case study which is about Cementi Victoria s.r.l., some investigations are considered including:

1. Computation of the lower heating value of sewage sludge that can be provided by Cuneo WWTP.
2. Choosing a most-fit solution for drying dewatered sewage sludge (transported from Cuneo WWTP) inside the Cementi Victoria cement plant.
3. Choosing a suitable rotary kiln burner, since the current burner under operation is almost obsolete and it is decided to be replaced by a new capable of alternative fuel burning.
4. Doing some practices using CFD methods to have an evaluation of DSS co-incineration in the rotary kiln in case of possible consequences including the co-incineration quality of DSS (influence in shape and quality of the flame, and temperature zones inside the kiln).

Before going through the above-mentioned topics, it must be noticed that another case study regarding the Cementi Victoria s.r.l containing a design of a solar greenhouse assisted with the radiant floor heating (just used in cold months, 8 months) for drying of dewatered sewage sludge was done in 2017. This is important since some comparisons will be investigated concerning this work in upcoming paragraphs.

### 4.1 Evaluation of the LHV of SS provided by Cuneo WWTP

Computing the Lower Heating Value (LHV) of dried sewage sludge is more straightforward using many approximation equations developed based on chemical composition to this end. Some of these equations have been brought below [12].

$$ul = 33,9.C + 120,12. (H - O/8) + 9,25.S - 2,51.H_2O \text{ MJ/kg}$$

$$ul = 33,9.C + 121,4. (H - O/8) + 10,5.S - 2,24.H_2O \text{ MJ/kg}$$

$$ul = 35.C + 94,3.H + 10,4.S + 6,3.N - 10,8.O - 2,44.H_2O \text{ MJ/kg}$$

considering an example of dried sewage sludge with humidity of 35% and the chemical composition of carbon C: 19.74%, oxygen O: 18.10%, nitrogen N: 1.98%, hydrogen H: 3.07%, sulfur S: 0.48 %, and 21.63 % of phosphorus and inorganic residue which are considered as constitutes of mineral substances, after calculation with equation 3 the LHV will be equal with 7,16987 MJ/kg [12].

Using these equations is only possible when there is a documentation providing the chemical composition of the sewage sludge. In case a WWTP like Cuneo that does not provide this kind of information, these equations can not be put in use. Cuneo WWTP provides documentation with only an indication of total organic carbon (TOC % S.S.; measured according to UNI EN 15936:2012) of dewatered sewage sludge which can be used to compute LHV value but with lower accuracy. Using the 5 datasheet reports provided by Cuneo WWTP regarding the dehydrated sewage sludge, the water and TOC content of each sample are summarized in table 11.

Table 11 Water and TOC content of the dewatered SS provided by Cuneo WWTP

Report number-Report date [m/y]	Water content [%t.q.]	TOC content [%s.s.]
1-01/2020	76.6	30.5 ± 11.4
2-04/2020	81.6	43.8 ± 16.4
3-07/2020	80.2	35.1 ± 13.2
4-11/2020	76.5	29.5 ± 11.1
5-05/2021	78.3	35.7 ± 13.4

As there is no indication of atomic composition of C, O, H, and S (in the provided datasheet) necessary to assess the LHV directly using the analytical equations, an experimental practice that relates LHV directly to TOC percentage by a linear equation can be used [26].

$$\text{LHV [kcal/kg dried basis]} = 96.2 \times \text{TOC [\% S.S. db]} + 53.7$$

To obtain this linear equation, the LHV was measured by a calorimetric method according to SR EN 15170:2009 and using the PARR 6200 calorimetric bomb and the TOC values by chromatographic method using the Thermo Scientific FlashEA 1112 Elemental Analyzer according to SR EN 15936: 2013 standard for 27 different dehydrated sewage sludge (25-40% water content and with a grain size of smaller than 200 µm) samples which were collected each month for two years from a WWTP. Also, the degree of interdependence between the two variables, the total organic carbon (TOC) and the lower heating value (LHV), was evaluated using the Pearson (r) linear correlation coefficient and the coefficient of determination R<sup>2</sup> which is the square of the correlation coefficient r. In both cases, the results show a very satisfactory performance for the linear equation [26].

Even though this equation seems strong enough but, to validate it, data from other sources were utilized., the data related to the dewatered sewage sludge (75.3% water content) of Rimini WWTP (440,000 PE) with Total Organic Matter (TOM) of 61.4% (dry basis) and LHV of 13.8 MJ/kg and the dewatered sewage sludge (79% water content) of Calderara di Reno WWTP (32,000 PE) with TOM of 55.1% (dry basis) and LHV of 10.7 MJ/kg and the dewatered sewage sludge (71.8% water content) of Forli WWTP (250,000 PE) with TOM of 55% (dry basis) and LHV of 12.4 MJ/kg were used to this end. The Lower Heating Values were measured using a Mahler calorimeter, according to EN 14918 [5].

Also, it seems there is a strong relationship between total organic carbon (TOC) and total organic matter (TOM) on a dry basis [27]. Having looked at the literature, the fraction TOM/TOC can be approximately considered equal to 1.8 [27],[28],[29],[30].

Computing TOC values (TOM/1.8) using the provided TOM values for three WWTPs (Rimini, Calderara di Reno, and Forli), the LHVs for dewatered sewage sludge using the linear equation [26] can be computed.

$$\text{LHV of dehydrated S.S. for Rimini WWTP} = 13.7 \text{ MJ/kg}$$

$$\text{LHV of dehydrated S.S. for Calderara di reno WWTP} = 12.3 \text{ MJ/kg}$$

$$\text{LHV of dehydrated S.S. for Forli WWTP} = 12.3 \text{ MJ/kg}$$

The results, using the equation [26], have a very good match with experimental results for Rimini and Forli WWTPs (<1% error) but with a higher error (13%) for Calderara di reno WWTP. So, using equation [26] seems to be suitable.

Using the equation [26] the LHV for the dehydrated sewage sludge samples (76.6% water content) of Cuneo WWTP considering the middle value for each report can be computed (on a dried basis). The results were shown in Table 12.

Table 12 LHVs of the SS provided by Cuneo WWTP (dry basis)

Sample number	LHV [MJ/kg]
1	12.5
2	17.8
3	14.3
4	12.1
5	14.6

Considering the mean value for LHVs which is 14.3 MJ/kg for Cuneo WWTP and the amount of approximately 500 kg/h (0.14 kg/s) of dried sewage sludge (23%wt water content) that can be produced by Victoria Cement s.r.l. by conductive-solar drying method [1], the weight of dry matter will be:

$$M_d = (1 - 0.23) \times 500 [\text{kg/h}] = 385 \text{ kg/h} = 0.11 \text{ kg/s}$$

And the Potential power that can be produced by burning DSS will be:

$$E_d = 0.11 [\text{kg/s}] \times 14.3 [\text{MJ/kg}] = 1.57 \text{ MW}$$

But part of this energy will be wasted to evaporate the water content (23%wt) of DSS which is:

$$2.26 [\text{MJ/kg}] \times 0.23 \times 0.14 [\text{kg/s}] = 0.07 \text{ MW}$$

So, the Net Power which can be obtained by burning DSS in the burner will be:

$$\text{Net Power} = 1.57 [\text{MW}] - 0.07 [\text{MW}] = 1.5 \text{ MW}$$

considering the approximate lower heating value of petcoke as equal to 30 MJ/kg, the degree of substitution of DSS based on LHV is equal to 180 kg/h of the petcoke. This means using the DSS can theoretically save 180 kg/h or 1,008 ton/year (operating time of 5,600 h/year) of the petcoke (this degree of substitution based on LHV practically never can be met due to incomplete conversion of DSS in the kiln burner flame). It is worth mentioning that burning this degree of DSS, also, strongly depends on the burner type which also may dictate using DSS with special quality (quantity, particle size, and so on).

## 4.2 A proposal for drying of SS in case of Cementi Victoria s.r.l.

It was decided to build a solar greenhouse assisted with radiant floor heating (conductive-solar mode) dryer in Cementi Victoria s.r.l plant (Figure 29, 30) for drying of the dewatered sewage sludge, meanwhile to evaluate the method from the economical and effectiveness point of view, a comparison with the most common solution in cement industries which is convective belt drying method was made.

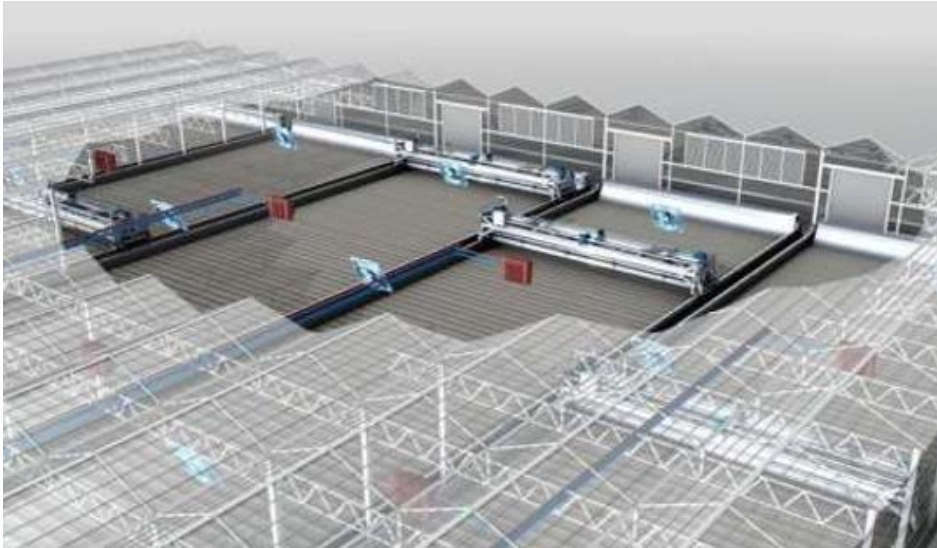


Figure 29 Greenhouse dryer [1]

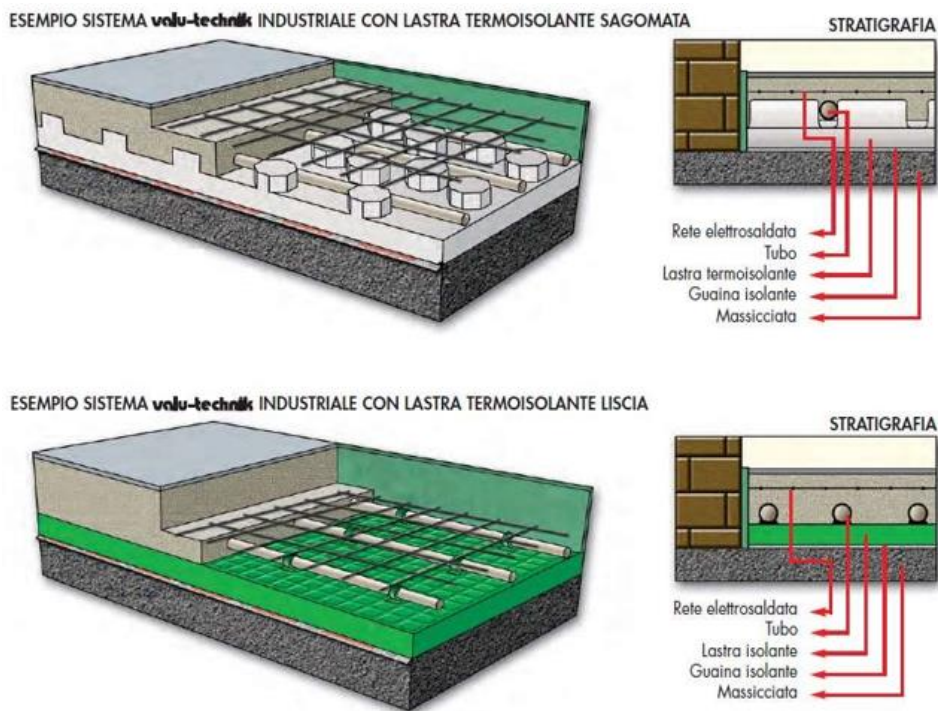


Figure 30 Radiant floor composition [1]

The Huber industry is one of the biggest companies that produce different types of sewage sludge drying machines. Huber Belt drier BT (low-temperature belt dryer) shown in Figure 31 being described by highest energy efficiency, full automation, very easy operation, compact, and sturdy stainless-steel design, low maintenance, and long life which meets all European and international standards besides generation of a dry, grainy, hygienic, safe, and easy to handle dried-product, can be a suitable belt dryer choice to be compared with solar greenhouse radiant floor assisted dryer.

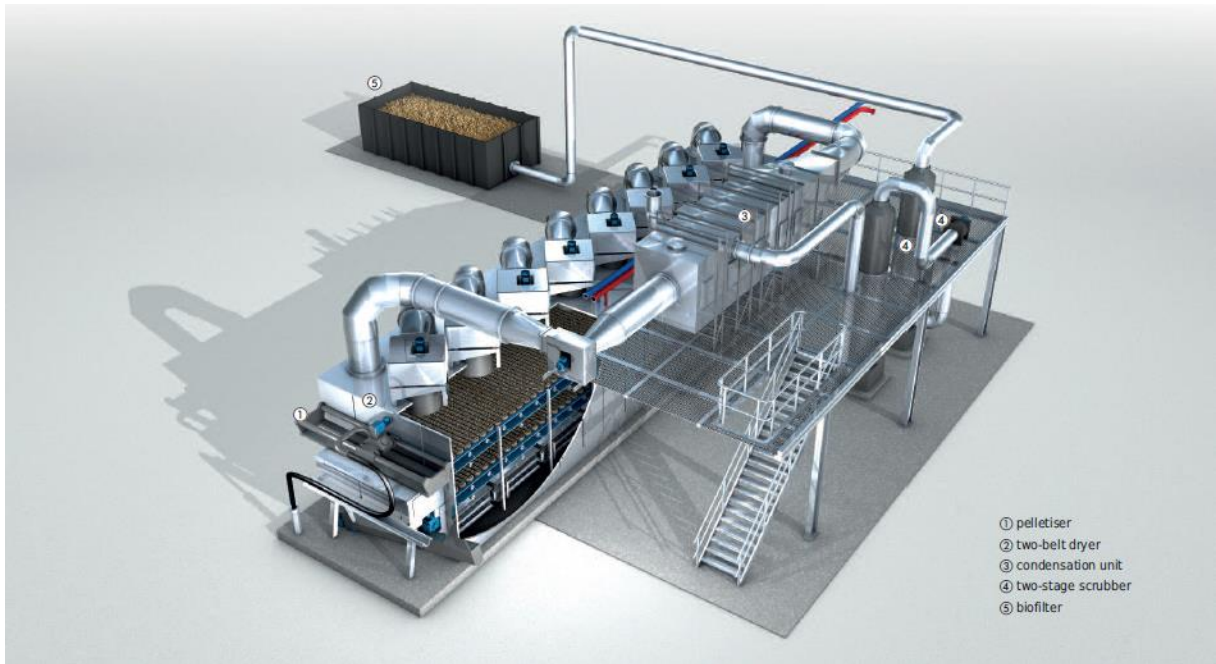


Figure 31 Huber belt dryer BT [1]

The available heat power which can be gained from Cementi Victoria s.r.l rotary kiln flue gas is equal to 1.9 MW considering the available time that this flue gas can feed sewage sludge dryer which is 5,600 h/y (the rotary kiln for the production of clinker is in operation about 7,560 h/y). The heat recovery using the hot fumes produced by the rotary kiln, however, cannot be carried out continuously because when the raw material grinding mill is in operation, the hot fumes are sent inside to operate the drying of the humid raw material and therefore the sludge drying process cannot be carried out. This mill is active at about 1,960 h/y which means 5,600 h/y is available for heat recovery. Assuming to exploit the waste heat for 8 months, a 3,800 h/y of operation of the supplementary heating floor for drying will be obtained, the available heat power in the scale of MWh/y will be:

$$1.9[\text{MW}] \times 5,600[\text{h/y}] = 10,640[\text{MWh/y}]$$

Having this power, the amount of water that can be evaporated using the Huber belt dryer BT considering that the reported specific thermal energy demand for this product by the producer is 0.8-0.85 kWh/kg<sub>wat</sub> (this number for the belt dryer in Schwenk, Karlstadt cement plant is also equal to 0.81 kWh/kg<sub>wat</sub>), will be:

$$10,640,000[\text{kWh/y}] \div 0.8 [\text{kWh/kg}_{\text{wat}}] = 13,300[\text{t}_{\text{wat}}/\text{y}]$$

This is much higher (around 77%) than the amount that could be evaporated using solar assisted radiant floor sludge drying method (7,500 t<sub>wat</sub>/y), partly because that the flue gas heat power used in the radiant floor heating system is utilized only for 3,800 h/y corresponding to 8 months instead of full availability of flue gas power which is 5,600 h/y corresponding to 12 months. This means leaving of around 1,800 h/y of flue gas power unused (corresponding for 4 months).

In the case of electrical energy demand, the greenhouse-radiant floor dryer (electrical energy demand of the heat recovery system is not included) also consumes a noticeable amount of electricity when compared to Huber belt BT. The electrical energy demand for Huber belt dryer BT is 0.03 and 0.15 kWh/kg<sub>wat</sub> for a capacity of dewatered sewage sludge of 0.3 and 6 t/h

respectively. For a throughput of 10,500 t/y of dewatered sewage sludge corresponding to 3800 h/y working hours which leads to a capacity of 2.76 t/h, the electric energy demand will be approximately 0.08 kWh/kg<sub>wat</sub> (considering a linear relationship between electrical energy demand and capacity for Huber belt drier). This is higher (51%) than the electrical energy demand for the solar greenhouse-radiant floor dryer.

Regarding the area necessary to accommodate the dryer, in the case of Huber belt dryer the length of the dryer is presented as 4 to 30 m compared to the greenhouse-radiant dryer which uses 100×60 m<sup>2</sup> of area. The difference in this regard is so much noticeable since if assuming the biggest possible Huber belt dryer with 30×10 m<sup>2</sup>, the necessary area for a greenhouse-radiant floor dryer is 20 times bigger.

In summary, having a specific amount of waste heat in hand (flue gas from the rotary kiln), the possible quantity of dewatered sewage sludge that can be treated is around 77% higher for Huber belt dryer but this dryer also demands around 51% higher electrical power than the greenhouse-radiant floor dryer. These data are summarized in Table 13.

Table 13 Solar drying greenhouse versus convective drying belt dryer

	<b>Greenhouse-radiant floor</b>	<b>Huber belt dryer BT</b>
<b>Ther. energy demand</b>	0.96 [kWh/kg <sub>wat</sub> ]	0.8-0.85 [kWh/kg <sub>wat</sub> ]
<b>Elec. energy demand</b>	0.053 [kWh/kg <sub>wat</sub> ]	0.03-0.15 [kWh/kg <sub>wat</sub> ]
<b>Medium</b>	Solar radiation-radiant floor	Waste heat from the kiln
<b>Occupied area</b>	6000 m <sup>2</sup>	At maximum 300 m <sup>2</sup>
<b>Initial investment cost</b>	3,295,000 €	?

Having this information in mind, it seems a belt dryer can be a good proposal for sewage sludge drying considering that it also occupies a smaller area. The decision for choosing a method for drying sewage sludge can be finalized considering very important factors which are the initial investment cost, maintenance cost, and operational cost.

### 4.3 Burner replacement

Due to the decision of cementi victoria s.r.l. for replacing their obsolete burner with a new one capable of co-firing of different waste fuels, a new multi-channel burner has opted to be replaced with the old one considering that the burner must be of the right dimensions for nominal operational capacity of the cement plant. The current burner has a capacity of 20,000,000 Kcal/h for a firing of pulverized petcoke of 30 t/d (not full capacity firing amount) and is assumed to be replaced by a ROTAFILAM<sup>®</sup> KGO burner from Pillard Feuerungen GmbH with a 35 MW capacity [31] (Figure 32).



Figure 32 ROTAFLAM® KGO burner from Pillard Feuerungen GmbH [31]

Since no specific datasheet for this product, unless its main dimensions [31] (total length = 1,560 cm, inside kiln length [max intrusive amount]= 965 cm, and outer diameter of the tip without refractory= 47 cm), could not be found; the present picture of this burner (Figure 31) was imported to Autocad® 2021 to obtain the necessary measurements of the burner face (a refractory of a 4.5 cm thickness is added to the outer burner shell). This dimensioning is shown in Figure 33. The inlet areas of the burner tried to be kept constant.

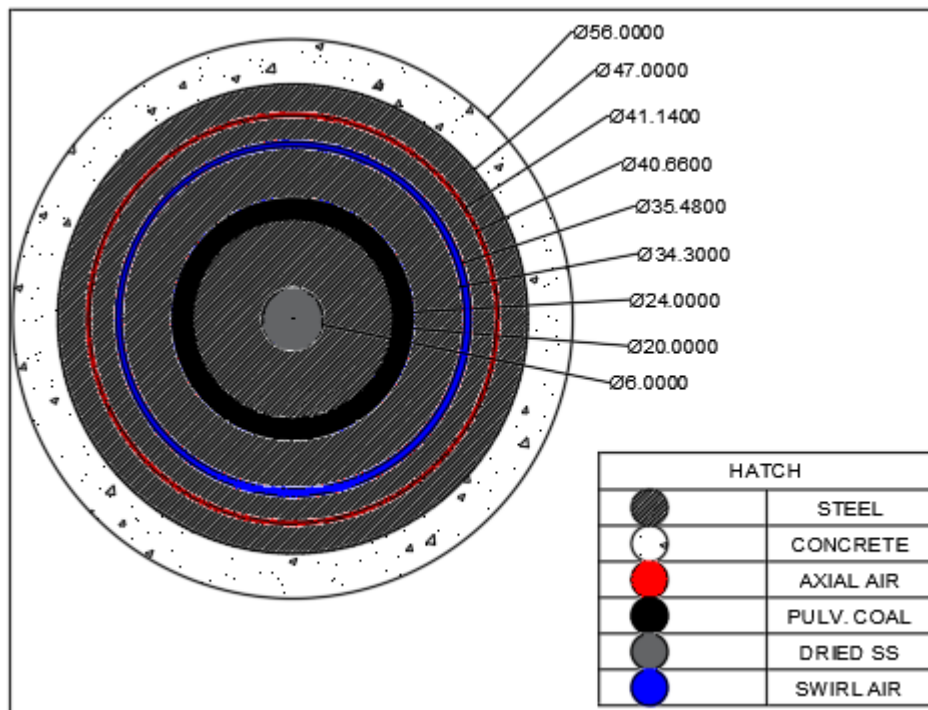


Figure 33 Dimensioning of the new ROTAFLAM® KGO burner face [cm]

$$\text{Area axial air inlet} = 3.0822e-3 \text{ m}^2$$

$$\text{Area swirl air inlet} = 6.4637e-3 \text{ m}^2$$

$$\text{Area petcoke inlet} = 13.816e-3 \text{ m}^2$$

$$\text{Area DSS inlet}=2.826\text{e-}3 \text{ m}^2$$

Since the swirl and axial momentum, and swirl number were not provided for this burner in literature, these numbers are imported from another paper at which a similar burner (similar heat power input for the burner) was utilized [32]. These numbers are 3.05 N/MW and 0.8 N/MW for the axial and swirl momentum respectively when the burner works with its maximum capacity. In the case that the burner works with lower power input, the axial and swirl momentum will drop for the burner. From the literature [32] the swirl and axial momentum equations (in N units) can be written as follow:

$$N_{ax}=\dot{m}_{sw}\times w_{sw,ax}+\sum\dot{m}_{tr+c}\times w_{tr+c}+\dot{m}_{ax}\times w_{ax} \text{ [N]}$$

$$N_{sw}=\dot{m}_{sw}\times w_{sw,sw} \text{ [N]}$$

In these equations  $\dot{m}_{sw}$ ,  $w_{sw,ax}$ ,  $\dot{m}_{tr+c}$ ,  $w_{tr}$ ,  $\dot{m}_{ax}$ ,  $w_{ax}$ , and  $w_{sw,sw}$  are swirl air mass flow rate, swirl air axial velocity component, the mass flow rate of fuel transporting air including the fuels, axial velocity of the fuels, the mass flow rate of the axial air, the velocity of the axial air and tangential velocity of swirl air respectively. Dividing obtained numbers ( $N_{ax}$ ,  $N_{sw}$ ) by the input power of the burner the swirl and axial momentum amount (in N/MW units) can be computed.

#### 4.4 Fuels

Taking into account the sewage sludge, an important consideration must be mentioned. Due to the huge variation of constituents amount (%ash, %volatile matter, %moisture, and %fixed carbon) in dried sewage sludge which by itself is due to the different raw composition (97 %wt of moisture) which differs from one city’s WWTP to another and the various processes that are done on the raw sewage sludge from initial treatments in the wastewater treatment plants to the final thermal drying processes that can differ from one case to another, choosing a specific composition for dried sewage sludge is nearly impossible, but, to do the simulation a composition data of proximate and ultimate analysis of sewage sludge were imported from [33]. Table 14 shows these data. From more than 35 types of sewage sludge introduced in [33], data related to the type SS9 which was more similar to the Cuneo provided sewage sludge from the heating value point of view, were considered.

Table 14 Ultimate and proximate composition of the chosen DSS

DSS	Ultimate analysis					Proximate analysis				HHV [Mj/kg]
	C%	H%	N%	S%	O%	M%	A%	VM%	FC%	
	%wt(dry ash-free basis)					%wt				
SS9	35.1	4.2	5	0.9	20.1	9.4	25.3	54.1	11.1	15.1

Regarding the main fuel which is the pulverized petcoke, composition data of proximate and ultimate analysis were imported from [34]. Table 15 shows these data.

Table 15 Ultimate and proximate composition of the chosen petcoke

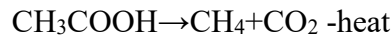
PC	Ultimate analysis					Proximate analysis				HHV [Mj/kg]
	C%	H%	N%	S%	O%	M%	A%	VM%	FC%	
	%wt(dry ash-free basis)					%wt				
PCJB	88.00	4.05	1.58	2.22	2.15	1.48	0.52	11.18	86.82	35.6

In most combustion environments, the reactions happen very fast and complex with many intermediate reactions. Considering this and that before combusting process initiation, solid fuels must be degraded into combustible gasses while moving in the flame jet, which this degradations by itself have very complex kinetics, the complexity of the problem even increases. All in all solid fuels combustion generally go through four stages: drying, devolatilization, burning of volatile substances, and burning of char

Considering data provided regarding the composition of the DSS and petcoke as fuels, it is evident that these two fuels can have very different behavior when combusted. This is first due to the far difference in the volatile matter and fixed carbon composition of these two and secondly due to the different devolatilization kinetics and products of volatile matter. Considering that the petcoke has a huge amount of char (mostly contains fixed carbon) which comes to exothermic reaction at high temperatures and slowly, this may result in the incomplete conversion of fixed carbon in the flame which may continue burning in the clinker bed causing local diffusion if the flame (and/or burner) is not managed properly or the fuel milled to big particles. Also, due to different particle sizes, densities, and compositions between these two fuels, the particles may follow a different jet path which by itself may distort the flame.

#### 4.4.1 DSS combustion kinetics

Regarding the DSS when used as fuel to be combusted, it follows generally 3 phases; 1- vaporization of remaining moisture 2- devolatilization and burning of volatiles, and 3- burning of char. The second phase may consist of devolatilized C<sub>2</sub>H<sub>6</sub> (ethane) and CH<sub>3</sub>-COOH (acetic acid) in the temperature range of 160-560 °C and 250-530 °C respectively with the peak temperature of devolatilization of roughly 320 °C and 300 °C respectively [35]. Even though in literature [36], these phases were neglected and the volatile burnout is directly addressed to CH<sub>4</sub> (methane) burning, but this can not be completely true because in reality there is burnout of ethane and decomposition of acetic acid partly to methane and carbon dioxide and partly to CH<sub>2</sub>CO (ketene) and water when the temperature goes higher than 440 °C. These decompositions were written below [37]:



The ketene itself is very reactive and unstable and reacting with other elements will be transformed to different products but since following the further reactions at which ketene will participate is very hard [39], this element is also removed from the simulation and decomposition of the acetic acid is just addressed to its decomposition to methane and carbon dioxide. During these decompositions, a considerable amount of energy will be exchanged which in the case of decomposition to the methane will be endothermic [39], but assuming that all the acetic acid just decomposes to methane and carbon dioxide, then the higher amount of methane production relative to the real case (two decompositions) and its following exothermic reaction with O<sub>2</sub> (oxygen) can justify removing both these decompositions from the simulation.

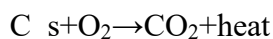
In this thesis, the volatile burnout was addressed to the burning of ethane and methane which is decomposed from acetic acid. Even though in literature [35, 38] other volatiles and/or oxides like CO, CO<sub>2</sub>, H<sub>2</sub>, HC, H<sub>2</sub>O, NH<sub>3</sub>, NO<sub>x</sub>, SO<sub>x</sub> (the last three mainly are considered pollutants) sometimes are considered, but in this work to prevent complexity and considering that most of this volatiles (except NH<sub>3</sub>, NO<sub>x</sub> and SO<sub>x</sub>) can be a by-product of main volatiles reactions and

decompositions (ethane and acetic acid), just burning of methane and ethane were assumed meaning that all volatile carbon is used to form a mixture of these two gases.

The combustion reactions of methane and ethane can possibly be defined by some intermediate reactions and intermediate active products like CO [36] but here to simplify the problem both gases (methane and ethane) were considered to burn in a single-stage mechanism. This assumption will not affect the final result to high orders because all these intermediate reactions happen very fast and interchangeably and also the heat released from the single-stage exothermic reaction considered is equal to the sum of the heat released or absorbed during exo-endo-thermic intermediate reactions. Hence, the final single-stage reactions can be written:



The third part of combustion was assigned to the char heterogeneous burning phase which starts after a complete burning of volatiles. In this phase, in the case of DSS, the char which mainly consists of ash (roughly 70 %wt) and fixed carbon (roughly 30 %wt) may have a limited degree of conversion in the flame and some particles may continue burning after a fall-off in kiln bed making local reducing condition [18]. The reaction concerning this phase can be written as a single-stage reaction to simplify the problem even though there are some intermediate reactions.



Having a feed rate of 500 kg/h (0.14 kg/s) of DSS and considering the results of ultimate and proximate analysis of chosen DSS, the feed rate (in %wt) of combustible elements including  $\text{C}_2\text{H}_6$ ,  $\text{CH}_4$ , and char must be computed to be exported to the simulation. This phase can be started with these computations:

$$\text{Ash}[\text{kg/s}]=0.14\times 0.253=0.0354 [\text{kg/s}]$$

$$\text{Fixed carbon or C}_s[\text{kg/s}]=0.14\times 0.111=0.0155 [\text{kg/s}]$$

$$\text{H}[\text{kg/s}]=0.14\times 0.042=0.0059 [\text{kg/s}]$$

$$\text{O}[\text{kg/s}]=0.14\times 0.201=0.0280 [\text{kg/s}]$$

$$\text{Volatile carbon}[\%wt]=35.1-11.1=24 [\%wt]$$

$$\text{Volatile carbon}[\text{kg/s}]=0.14\times 0.24=0.0336[\text{kg/s}]$$

The volatile carbon content which is included in acetic acid and ethane can be estimated by two equations. The first one can be written using the oxygen content and the second one using the volatile carbon content of the gaseous stream. The mass fraction of O/C in each molecule of acetic acid ( $\text{CH}_3\text{COOH}$ ) is 4/3. if the carbon content included in the acetic acid and ethane structure is expressed by x, y respectively then equations can be written as follows:

$$x+y=0.0336 [\text{kg/s}]$$

$$4x/3=0.0280 [\text{kg/s}]$$

solving these equations, x, y can be obtained 0.0210, 0.0126 [kg/s] respectively. these show the total amount of carbon included in acetic acid and ethane respectively. this means that the inlet mass flow rate of acetic acid and ethane can be computed:

$$\text{CH}_3\text{COOH} [\text{kg/s}] = x + x/6 + 4x/3 = 0.0525 [\text{kg/s}]$$

$$\text{C}_2\text{H}_6 [\text{kg/s}] = y + y/4 = 0.0158 [\text{kg/s}]$$

But as mentioned before, it was assumed that all acetic acid decomposes to methane and carbon dioxide. Hence the mass flow rate of methane will be:

$$\text{CH}_4 = 16/60 \times 0.0743 = 0.0140 [\text{kg/s}]$$

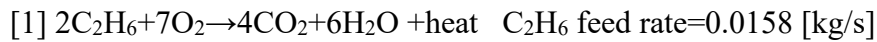
But checking the value of H necessary to form ethane and methane:

$$\text{Necessary H to form ethane and methane} [\text{kg/s}] = x/6 + y/4 = 0.0066 [\text{kg/s}]$$

$$\text{Necessary H to form ethane and methane} [\% \text{wt}] = (0.0066/0.14) \times 100 = 4.75 [\% \text{wt}]$$

This means to have ethane and methane with the computed value, a higher percentage of H (4.75-4.2=0.55%) must be present in the DSS structure, but considering that this higher percentage is just about 13% of the reported value for H, this problem can be ignored.

Now, simplifying all the abovementioned expressions, there are 3 combustion reactions at which the feed rate of reactants can be as follow:



$$\text{Combustible char: } \text{C}_s / (\text{Ash} + \text{C}_s) = 0.3045$$

$$\text{Char particles diameters} = 1-2 \text{ mm}$$

#### 4.4.2 petcoke combustion kinetics

Petcoke, the main fuel, has a very different composition rather than DSS having a higher percentage of char (which mostly consists of fixed carbon) and a lower percentage of volatiles. The number of papers in literature to describe the devolatilization kinetics of petcoke is negligible may be due to a negligible amount of volatiles in the petcoke. Considering the data provided in Table 15, the volatile compounds containing carbon can be negligible too (1.38 %wt of C). Because a lower amount of total heat released during the combustion of petcoke is provided by volatile combustions, then this phase can be simplified as much as possible. In this work, it is assumed that all carbon included in volatiles is in the form of CH<sub>4</sub> (methane), and the remaining hydrogen and oxygen form H<sub>2</sub> and pollutant oxides like SO<sub>x</sub> and NO<sub>x</sub> molecules respectively. All the reactions of molecules containing N, S atoms are neglected as they release/absorb a lower amount of energy when they react, and their lower concentration.

Considering the mono combustion, the feed rate of petcoke will be about 1250 kg/h (0.35kg/s) [banche] which in the case of co-firing with DSS this value will decrease with the following amount (Table 15, 16):

$$\text{Amount of replaceable DSS based on HHV} = (15.1[\text{MJ}]/35.6[\text{MJ}]) \times 0.14 [\text{kg/s}] = 0.0594 [\text{kg/s}]$$

$$\text{Feed rate of the petcoke in case of co-firing with DSS} = 0.35 - 0.0594 = 0.2906 [\text{kg/s}]$$

To investigate the effect of DSS co-firing two cases can be defined, the mon firing case and the co-firing case.

**In the first case**, the mass flow rates will be:

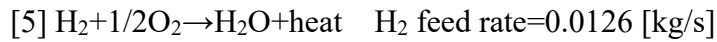
$$\text{CH}_4 \text{ [kg/s]} = 0.35 \times (0.0138 + 0.0138/3) = 0.0064 \text{ [kg/s]}$$

$$\text{H}_2 \text{ [kg/s]} = 0.35 \times (0.0405 - 0.0138/3) = 0.0126 \text{ [kg/s]}$$

$$\text{Ash} = 0.35 \times 0.0052 = 0.0018 \text{ [kg/s]}$$

$$\text{C}_s = 0.35 \times 0.8682 = 0.3039 \text{ [kg/s]}$$

The main reactions neglecting the intermediate reactions are:



$$\text{Combustible char: } \text{C}_s / (\text{Ash} + \text{C}_s) = 0.9941$$

$$\text{Char particles diameters} = 0.1 - 1 \text{ mm}$$

The feed rate of hot air to perform mono-combustion of petcoke (reactions 4, 5, 6) will be equal to:

$$\text{O}_2 \text{ required [kg/s]} = 0.0064 \times (64/16) + 0.0126 \times (16/2) + 0.3039 \times (32/12) = 0.9364 \text{ [kg/s]}$$

Considering 5% extra oxygen the required oxygen will be 0.98 [kg/s]

And finally the feed rate of hot air considering its composition of 23%wt of O<sub>2</sub> and 77%wt of N<sub>2</sub> will be:

$$\text{Hot air [kg/s]} = 4.35 \times 0.98 = 4.26 \text{ [kg/s]}$$

**In the second case**, the mass flow rates will be:

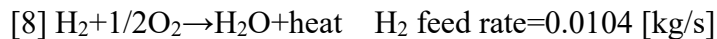
$$\text{CH}_4 \text{ [kg/s]} = 0.2906 \times (0.0138 + 0.0138/3) = 0.0053 \text{ [kg/s]}$$

$$\text{H}_2 \text{ [kg/s]} = 0.2906 \times (0.0405 - 0.0138/3) = 0.0104 \text{ [kg/s]}$$

$$\text{Ash} = 0.2906 \times 0.0052 = 0.0015 \text{ [kg/s]}$$

$$\text{C}_s = 0.2906 \times 0.8682 = 0.2523 \text{ [kg/s]}$$

The main reactions neglecting the intermediate reactions are:



The feed rate of hot air to perform mono-combustion of petcoke (reactions 1, 2, 3, 7, 8, 9) will be equal to:

$$\text{O}_2 \text{ required [kg/s]} = 0.0158 \times (224/60) + 0.0140 \times (64/16) + 0.0155 \times (32/12) + 0.0053 \times (64/16) + 0.0104 \times (16/2) + 0.2523 \times (32/12) = 0.9335 \text{ [kg/s]}$$

Considering 5% extra oxygen the required oxygen will be 0.98 [kg/s]

And finally the feed rate of hot air considering its composition of 23%wt of O<sub>2</sub> and 77%wt of N<sub>2</sub> will be:

$$\text{Hot air [kg/s]}=4.35\times 0.98=4.26 \text{ [kg/s]}$$

In the literature [41] for the fuel conveying air, a mass flow rate of 0.35 to 0.82 of the fuel mass flow rates is considered with a bigger fuel conveying mass flow rate for the secondary fuel. In this work DSS conveying air and petcoke conveying air mass flow rates considered 0.45 of the DSS mass flow rate (0.063 kg/s) and 0.35 of the petcoke mass flow rate (0.1225 kg/s for mono-firing and 0.1017 kg/s in case of the co-firing case) respectively.

To obtain a logical amount for swirl and axial air velocities considering their importance to be assigned into their respective boundaries and knowing that some of these parameters can be proposed by the burner producer and some others can be optimized by the operator of the burner during the operation, in this work to prevent too many trials with these parameters and avoid complicated fluid dynamics computation and meanwhile to have logical values, data of other papers [40, 41, 42] were used to initialize the iterations for finding the best configuration of the inlet mass flow rates and velocities combination which provides a better characteristic of the flame.

## 4.5 CFD analysis

In this section, a computational fluid dynamic (CFD) analysis of the dried sewage sludge co-combustion inside the rotary kiln was done to investigate the effect of DSS addition as a secondary co-fuel. Some simplifications were made to make the model consistent and simple in terms of computational cost. The goal is that to have a provision of possible effects of DSS co-firing in temperature zones inside the kiln and the flame shape and temperature. To this end, a simulation of mono-incineration of petcoke was also done to be compared with a co-incineration case with DSS.

### 4.5.1 Geometry

The Geometry was designed by a 3d modeling of the kiln currently used in Cementi Victoria s.r.l. and the proposed burner (ROTAFLAM<sup>®</sup> KGO) in the SpaceClaim module of ANSYS WORKBENCH. Some simplifications are made which is expected to have not a considerable effect on the results which are looked for. These simplifications were:

1. The kiln was assumed to be still and not rotating
2. The kiln inclination was assumed to be zero which has a 4% of inclination in reality
3. The kiln shell was assumed to be of 82 m length, 2.4 m inner diameter, and 5cm thickness and built with stainless steel
4. The intrusion amount of the burner head inside the kiln is assumed to be 1 m, then the simulation was done from the burner tip meaning that the kiln was considered from the burner tip and with 81 m (82-1 m) length.
5. The burner was assumed to be concentric with the kiln and at the same alignment with it.
6. The burner was assumed to be built with stainless steel

### 4.5.2 Meshing

The meshing of the 3d model designed in the SpaceClaim module was done in the ANSYS MESHING TOOL with automatic standard mesh (Figure 34). The total number of cells were equal to 2,264,889.

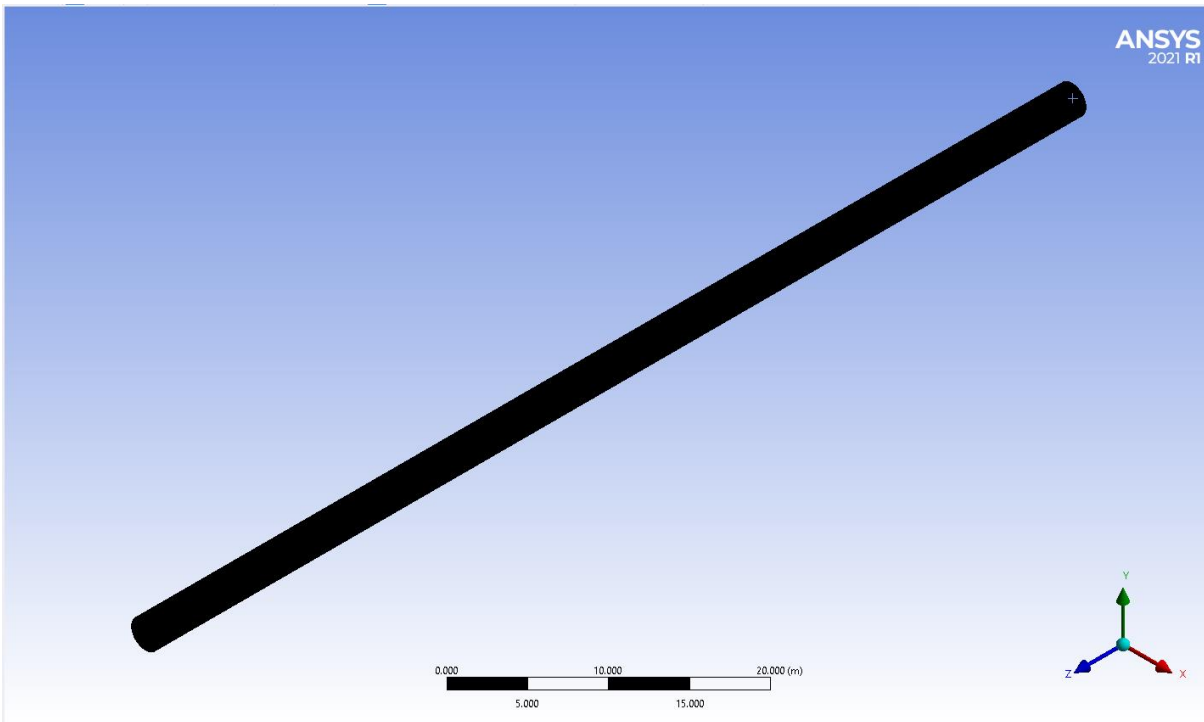


Figure 34 Rotary kiln and burner after meshing in ANSYS MESHING TOOL

### 4.5.3 Setup

The mass, momentum, and energy equations were solved in steady-state form. The simulation was done with the pressure based solver. The effect of gravity was considered. For the fluid dynamic viscosity effects the standard k- $\epsilon$  model with standard wall functions were considered. For the radiation, P1 model was chosen. To model combustion, species transport model with mixture template and with volumetric reactions (to model volumetric reactions of methane, ethane and hydrogen gasses) and particle surface reactions (to model char heterogeneous combustion; char particles were fed by discrete phase modeling (DPM) interacting with gaseous stream) were used. For the Turbulence-chemistry interaction, the finite rate/eddy dissipation model was used to take both laminar and turbulent effects into consideration depending on the flow behavior. In the mixture material section all reactants and products involved in reactions were defined with their reaction exponent order and also with Arrhenius coefficients (frequency factor and activation energy) for each reaction.

#### 4.5.3.1 Boundary conditions

Boundary conditions can be divided into fluid dynamics and energy boundaries. For the fluid dynamics problem, the following boundaries are defined:

1. The inlet mass flow rates for the petcoke and DSS containing their fuel transporting air mass flow rates for fuel feed channels
2. The inlet velocity for the swirl (tangential and axial component 5 and 40 m/s respectively) and axial air (45 m/s) feed channels
3. The inlet mass flow rate for the hot air (secondary air) feed channel
4. The pressure outlet for the kiln feed mouth (a negative pressure of 200 pascal assumed to be created with an ID fan)
5. The no-slip wall boundary condition for the kiln wall and all areas of the burner which is in contact with fluid

For the Energy problem, the following boundaries are defined:

1. The inlet temperature of petcoke and DSS containing their fuel transporting air was considered 323K considering a preheating treatment of transporting air to raise the fuel stream temperature to 50 K.
2. For the secondary hot air, an inlet temperature of 1173 K was considered, this air as mentioned before was preheated by contacting with hot clinker (after discharge from the kiln) before entering the kiln [43].
3. The primary airs including axial and swirl air were assumed to enter the kiln with an inlet temperature of 323 K.
4. The kiln walls are considered adiabatic [40].

#### 4.5.4 Results and discussion

A simulation considering the above-mentioned boundary conditions was done for co-firing of pulverized DSS with petcoke (second case) to investigate the flame quality obtained using the chosen burner (Figure 35, 36). The results as could be expected do not show a proper flame with long and thin-high momentum shape. The reason why this happens can be described according to the literature [18] that explains the most proper burner to facilitate kilns with very long and small diameter geometry like something currently is under operation in Cementi Victoria s.r.l. are those with a single channel to feed fuel and primary air (first generation burners) together and without dedicated channels for axial and swirl air. The second reason can be addressed for the difficulty of regulating different inputs for boundary conditions like the inlet velocities of axial air and swirl air where a small change of each of these inputs can dramatically change the flame shape. It is very likely to obtain a suitable flame regulating these input parameters precisely but since this needs too much effort from the computational cost point of view, finding a good set up of these parameters could not be successful. Other than the parameters presented, the results show a very strong correlation with the excessive amount of hot secondary air mass flow rate which can be changed from 0.05 to 0.25 of the necessary air. Also the type of simulation that is done by the Ansys fluent which dictates the separation of char solid combustion from volumetric volatile combustion can also be a source of problem. Due to the fair results obtained for the second case of co-firing, simulation for the mono-firing of petcoke (first case) was not conducted.

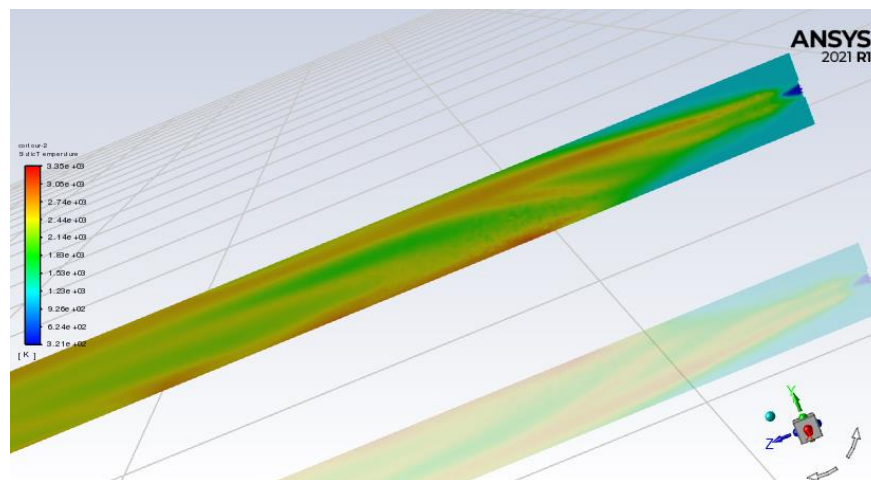


Figure 35 Flame shape and temperature

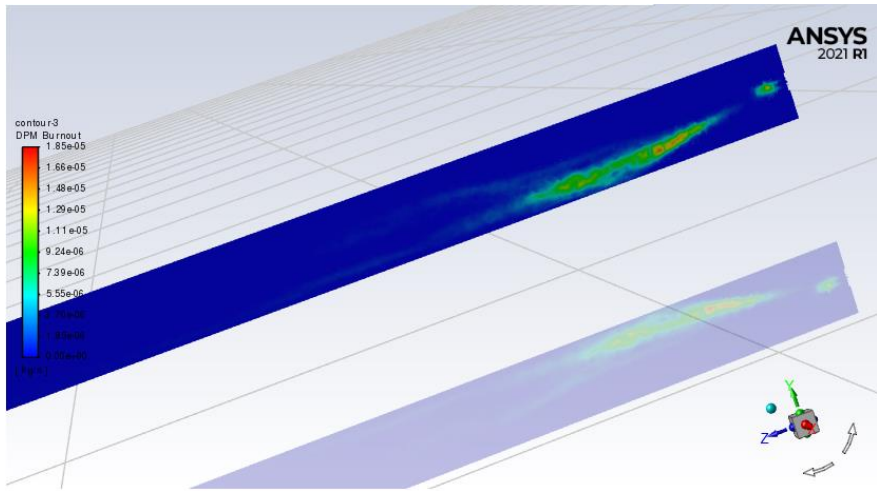


Figure 36 Char burn out quantity and path

## 5 Conclusion

In conclusion, this thesis work aimed at providing some information on sewage sludge usage in the cement industry including the different drying methods using heat recovery of flue gases produced in the kiln during the production process of clinker and investigation of possible usage of sewage sludge after drying as a fuel agent. Many technological ways and practical experiences were introduced for the end of drying of sewage sludge and also many investigations were done in order to obtain a good provision of dried sewage sludge co-firing possibility in the cement rotary kilns.

For the drying purpose, an alternative method of convective belt drying was introduced and compared with the way which was decided to be used in Cementi Victoria s.r.l (greenhouse-radiant floor dryer) and the benefits and drawbacks of each method were explained.

As mentioned in the literature and the part regarding the case study of the Cementi Victoria s.r.l using dried sewage sludge as a co-fuel, if it is co-fired to a limited degree, can be a suitable choice for cement factories because while helping ecological disposal of sewage sludge, a good sustainable source of thermal energy will be accessible for them.

## 6 References

- [1] Banche, A. Recupero di cascami termici derivanti dalla produzione di clinker per la realizzazione di un processo di essiccamento fanghi [Master's Thesis, Politecnico di Torino]
- [2] Schnell, Matthias, Thomas Horst, and Peter Quicker. "Thermal treatment of sewage sludge in Germany: A review." *Journal of environmental management* 263 (2020): 110367.
- [3] Bennamoun, Lyes, Patricia Arlabosse, and Angélique Léonard. "Review on fundamental aspect of application of drying process to wastewater sludge." *Renewable and Sustainable Energy Reviews* 28 (2013): 29-43.
- [4] Li, Yeqing, et al. "The industrial practice of co-processing sewage sludge in cement kiln." *Procedia Environmental Sciences* 16 (2012): 628-632.
- [5] Bianchini, A., et al. "Sewage sludge drying process integration with a waste-to-energy power plant." *Waste management* 42 (2015): 159-165.
- [6] Tańczuk, Mariusz, Wojciech Kostowski, and Marcin Karaś. "Applying waste heat recovery system in a sewage sludge dryer—A technical and economic optimization." *Energy Conversion and Management* 125 (2016): 121-132.
- [7] Lin, Yiming, et al. "Utilization of municipal sewage sludge as additives for the production of cement." *Journal of hazardous materials* 213 (2012): 457-465.
- [8] Fang, Ping, et al. "Using sewage sludge as a denitration agent and secondary fuel in a cement plant: A case study." *Fuel Processing Technology* 137 (2015): 1-7.
- [9] Świerczek, Lesław, Bartłomiej Michał Cieślik, and Piotr Konieczka. "Challenges and opportunities related to the use of sewage sludge ash in cement-based building materials—a review." *Journal of Cleaner Production* (2020): 125054.
- [10] Slim, Rayan, Assad Zoughaib, and Denis Clodic. "Modeling of a solar and heat pump sludge drying system." *International journal of refrigeration* 31.7 (2008): 1156-1168.
- [11] Di Fraia, Simona, et al. "Energy, exergy and economic analysis of a novel geothermal energy system for wastewater and sludge treatment." *Energy Conversion and Management* 195 (2019): 533-547.
- [12] Neamt, Ioan, and Ioana Ionel. "Environmental management of the sewage sludge: case study—the wastewater treatment plant of Timisoara." *Technical Gazette* 3 (2013): 435-439.
- [13] Di Fraia, Simona, et al. "An integrated system for sewage sludge drying through solar energy and a combined heat and power unit fuelled by biogas." *Energy Conversion and Management* 171 (2018): 587-603.
- [14] Ploteau, Jean-Pierre, et al. "Sludge convection drying process: Numerical modeling of a heat pump assisted continuous dryer." *Drying Technology* (2019).
- [15] Di Fraia, S., et al. "Thermo-economic analysis of a novel cogeneration system for sewage sludge treatment." *Energy* 115 (2016): 1560-1571.
- [16] Moses P.M. Chinyama (August 9th 2011). *Alternative Fuels in Cement Manufacturing*, Alternative Fuel, Maximino Manzanera, IntechOpen, DOI: 10.5772/22319. Available from: <https://www.intechopen.com/chapters/17593>

- [17] Schorcht F, Kourti I, Scalet B, Roudier S, Delgado Sancho L. Best Available Techniques (BAT) Reference Document for the Production of Cement, Lime and Magnesium Oxide: Industrial Emissions Directive 2010/75/EU:(Integrated Pollution Prevention and Control). EUR 26129. Luxembourg (Luxembourg): Publications Office of the European Union; 2013. JRC83006
- [18] Nørskov, L. K., Dam-Johansen, K., Glarborg, P., Jensen, P. A., & Larsen, M. B. (2012). Combustion of solid alternative fuels in the cement kiln burner. Kgs. Lyngby: Technical University of Denmark (DTU).
- [19] ECRA (2016) Evaluation of the energy performance of cement kilns in the context of co-processing. 1039, European Cement Research Academy, Duesseldorf.
- [20] "Construction and operation of a Sewage sludge thermal drying process at low temperature using the clinker kiln gases in Cemex Alicante cement factory AQUALOGY." (2013).
- [21] Available online: <https://www.andritz.com/separation-en/references/reference-cases/success-story-schwenk-cement>
- [22] Trenkwalder, J. (2010). Waste heat recovery for the drying of sewage sludge. 8. 48-53.
- [23] Diener, S., Reiser, J.C., Mbéguéré, M., Strande, L., 2012, Waste heat recovery from cement production for faecal sludge drying, Eawag: Swiss Federal Institute of Aquatic Science and Technology, Dübendorf, Switzerland
- [24] Đurđević, Dinko, Paolo Blecich, and Željko Jurić. "Energy recovery from sewage sludge: The case study of Croatia." *Energies* 12.10 (2019): 1927.
- [25] Available online: <https://archive.org/details/HolderbankCementEngineeringBook>
- [26] Serbanescu, A., Barbu, E., Nicolescu, I., & Bucur, E. (2017). Interdependence between total organic carbon content and heating value of sewage sludge samples.
- [27] Jiménez, E. I., & García, V. P. (1992). Relationships between organic carbon and total organic matter in municipal solid wastes and city refuse composts. *Bioresource Technology*, 41(3), 265-272.
- [28] Darwish, K. M. (2020). Evaluation of Sludge Properties in Sewage Sludge from Guarchia Wastewater Treatment Plant in Benghazi-Libya. *Journal of Material Sciences & Manufacturing Research*. SRC/JMSMR/110, 3.
- [29] Zoghalmi, R. I., Hamdi, H., Mokni-Tlili, S., Hechmi, S., Khelil, M. N., Aissa, N. B., ... & Jedidi, N. (2020). Monitoring the variation of soil quality with sewage sludge application rates in absence of rhizosphere effect. *International Soil and Water Conservation Research*, 8(3), 245-252.
- [30] Jakubus, M. (2020). Changes in lead and chromium contents in sewage sludge evaluated using both single extractants and sequential method. *Environmental Pollutants and Bioavailability*, 32(1), 87-99.
- [31] Available online: <http://cementassociation.ir/Library/313.pdf>
- [32] Liedmann, B., Wirtz, S., Scherer, V., & Krüger, B. (2017). Numerical study on the influence of operational settings on refuse derived fuel co-firing in cement rotary kilns. *Energy Procedia*, 120, 254-261.
- [33] Król, K., Iskra, K., Ferens, W., & Miodoński, J. M. (2019). Testing properties of sewage sludge for energy use. *Environment Protection Engineering*, 45(4).
- [34] Gao, F., Liu, J., Wang, C., Zhou, J., & Cen, K. (2012). Effects of the physical and chemical properties of petroleum coke on its slurrability. *Petroleum Science*, 9(2), 251-256.

- [35] Hernández, A. B., Okonta, F., & Freeman, N. (2017). Thermal decomposition of sewage sludge under N<sub>2</sub>, CO<sub>2</sub> and air: Gas characterization and kinetic analysis. *Journal of environmental management*, 196, 560-568.
- [36] Wang, Y., & Yan, L. (2009). CFD based combustion model for sewage sludge gasification in a fluidized bed. *Frontiers of Chemical Engineering in China*, 3(2), 138-145.
- [37] Cavallotti, C., Pelucchi, M., & Frassoldati, A. (2019). Analysis of acetic acid gas phase reactivity: Rate constant estimation and kinetic simulations. *Proceedings of the Combustion Institute*, 37(1), 539-546.
- [38] Žnidarčič, A., Katrašnik, T., Zsély, I. G., Nagy, T., & Seljak, T. (2021). Sewage sludge combustion model with reduced chemical kinetics mechanisms. *Energy Conversion and Management*, 236, 114073.
- [39] Nguyen, M. T., Sengupta, D., Raspoet, G., & Vanquickenborne, L. G. (1995). Theoretical study of the thermal decomposition of acetic acid: decarboxylation versus dehydration. *The Journal of Physical Chemistry*, 99(31), 11883-11888.
- [40] Ariyaratne, W. H., Malagalage, A., Melaaen, M. C., & Tokheim, L. A. (2015). CFD modelling of meat and bone meal combustion in a cement rotary kiln—Investigation of fuel particle size and fuel feeding position impacts. *Chemical Engineering Science*, 123, 596-608.
- [41] Pieper, C., Wirtz, S., Schaefer, S., & Scherer, V. (2021). Numerical investigation of the impact of coating layers on RDF combustion and clinker properties in rotary cement kilns. *Fuel*, 283, 118951.
- [42] Wirtz, S., Pieper, C., Buss, F., Schiemann, M., Schaefer, S., & Scherer, V. (2020). Impact of coating layers in rotary cement kilns: Numerical investigation with a blocked-off region approach for radiation and momentum. *Thermal Science and Engineering Progress*, 15, 100429.
- [43] Wang, S., Lu, J., Li, W., Li, J., & Hu, Z. (2006). Modeling of pulverized coal combustion in cement rotary kiln. *Energy & Fuels*, 20(6), 2350-2356.